Astrophysical Consequences of Phase Transition in Millisecond Pulsars

Thesis report submitted in partial fulfillment of the requirements

for the degree of

Bachelor of Science in Physics

by

Aspradakis Nikolas

under the supervision of

Dr John Antoniadis

Department of Physics
University of Crete
February 26, 2024

Abstract

In a low mass binary system with a neutron star as the primary star and a star in the main sequence phase as its companion, after the end of the accretion process, where we have a MSPs-WD system, the orbit due to tidal forces should be almost circular with eccentricity equal to zero. However the observations of some eccentric binaries have shown that something making the system to have a more elliptical orbit with $e \simeq 0.1$. The explanation we will try to give here is based on the theory of strange stars and the phase-transition from baryonic matter to quark matter which causes an asymmetric kick that disrupts the system and changes the eccentricity of the orbit. We want to have a better understanding to what is the relationship between the the mass and radius of a neutron star in order to have the phase-transition from the different layers of the pulsar's core.

In order for us to investigate this phenomena, we will use a software program called MESA, that can simulate the stellar evolution of a star, or in our case a binary system of a neutron star and a main sequence star that will eventually evolve in a millisecond pulsar-white dwarf system. This simulation will provide us with information regarding the quantities that we are interested (mass, radius, spin period etc). After collecting the necessary data, we will import them to the evolution code concerning the spin evolution, the mass transfer process and the accretion torque mechanism that we wrote on using python, we proceeded with further analysis for this project.

In the first chapter we present a thorough theoretical background about stellar evolution, binary evolution and phase transition from baryonic matter to quark matter. At the end of this chapter there will be a brief talk about the purpose of the thesis. In the second chapter we discuss about the numerical tools and the code about the evolution of the binary we want to study through the simulation that MESA can provide. There will be a discussion about the polytropic equation of state that we choose to use, the evolution of angular momentum, the spin evolution and the parameters we used. We will also analyze the accretion process and torque provided by both Tauris and Bhattacharyya. In the third chapter we will present the results of this analysis and compare the different cases we chose to study. To finish the thesis, in the final chapter we present the conclusions regarding the project and a brief discussion about future projects and changes to make the analysis more clear and correct problematic parts.

Contents

List of Figures

Chapter 1

Introduction

This chapter presents a theoretical overview that is necessary to know for understanding this project. In more detail, the *evolution of a star* and its fate depending on the mass of the star will be discussed. Also, the nature of *neutron stars* and fundamental properties such as the *equation of state* will be presented. Furthermore, the chapter will mention what happens when the star or, in this case, the neutron star belongs to a binary system and what changes during the evolution process. To finish this chapter, the text will illuminate the reader about the actual purpose of this thesis and what follows in the next chapter.

1.1 Stellar evolution

Stellar evolution refers to the transformation of a star throughout its lifespan, from its inception to its ultimate demise. The specifics of stellar evolution can differ based on a star's mass, but here is a general overview [Iben Jr, 1967]. The chapter will begin by examining the stellar evolution of a single star. Following that, attention will be expanded to include the evolution of a binary system (see Section 1.2).

1.1.1 Important Properties of Stellar Evolution

A crucial factor in the evolution of a star is **the evolution of the star radius**. Using the Stefan-Boltzman law we can calculate the radius by rearranging the equation for the luminosity of a star and we can estimate its place in the H-R diagram (Hertzsprung-Russell) [Carroll and Ostlie, 2017]:

$$L = 4\pi R^2 \sigma T_{\text{eff}}^4 \Rightarrow R = \sqrt{\frac{L}{4\pi T_{\text{eff}}^2}} \tag{1.1.1}$$

where L is the luminosity, σ is the Stefan-Boltzman constant and T_{eff} is the effective temperature of the star. The radius evolution is linked with stellar evolution as it changes as the star enters a different phase in its lifespan and portrays a central roll in the ***mass transfer process***, (see Section 1.2.2).

In order to better understand this whole process we need to study the different areas of equilibrium. To be more precise we need *Stellar Timescales*. Three crucial time scales pertain to the evolution of a star, each tied to alterations in its structural mechanics, thermal characteristics, and elemental composition [Pols, 2011].

Dynamical timescale: The dynamical timescale refers to how quickly a star responds to a perturbation that disrupts its state of hydrostatic equilibrium. Also this timescale is generally on the order of hours or even less and it is given by the following equation:

$$\tau_{dyn} \simeq \sqrt{R^3/GM} \tag{1.1.2}$$

Thermal timescale: The thermal timescale defines the speed at which alterations in a star's thermal structure can take place. Consequently, it also represents the timescale on which a star in thermal equilibrium responds when its thermal equilibrium is disrupted. We can calculate it following this equation:

$$\tau_{th} \simeq GM^2/RL \tag{1.1.3}$$

Nuclear timescale: Thermal equilibrium is not disturbed as the nuclei fuel is abundant. The time span associated with this process is known as the nuclear timescale. Because nuclear fuel is consumed

and transformed into other elements, this timescale also signifies how quickly changes in the star's interior composition happen and the below equation can provide this time scale:

$$\tau_{nuc} \simeq E/L \propto Mc^2/L \tag{1.1.4}$$

To summarize stellar evolution provides insights into the life cycle of stars, element production, and its significance for understanding galaxy evolution, planetary system formation, and binary evolution.

Simple Definition of a Star

A star is a luminous sphere of hot gas held together by gravity, producing light through nuclear fusion in its core. It is a fundamental component of galaxies and plays a crucial role in creating elements and shaping the universe. A more analytical exploration of star formation is provided by [McKee and Ostriker, 2007], although the main stages of this process will be mentioned in the following subsection.

1.1.2 Formation of a Star

The star formation process combines both regular physical principles and random factors, resulting in a diverse range of stars and stellar systems with unique properties and characteristics. In galaxies, the formation of stars is a complex process influenced by various factors. Initially, interstellar matter tends to condense into star-forming regions, but galactic tidal forces pose a counteracting influence, restricting star formation to areas with sufficient gas density. On smaller scales, thermal pressure emerges as the primary force resisting gravity, setting a minimum mass requirement for a cloud core to collapse and initiate star formation (Jeans mass, M_J), initially giving birth to a *protostar* [Carroll and Ostlie, 2017]. These protostars grow by accreting surrounding material. Magnetic fields are involved in mediating gas accretion onto protostars and launching bipolar jets during the birth of new stars.

Within giant molecular clouds, turbulence and magnetic fields prevent gas from collapsing into stars. Turbulence maintains gas motion, while magnetic fields influence its dynamics [Larson, 2003]. So basically stars begin as clouds of gas and dust in space.

In regions where stars are born, it's common for them to form as part of binary systems (see Section 1.2), or within clusters where several stars are gravitationally connected. The process of stars forming from collapsing gas and dust clouds relies heavily on the redistribution of angular momentum. In densely populated areas, interactions among stars happen more frequently and intensely. These interactions can lead to direct collisions or mergers between stars. Particularly in dense environments, these interactions are believed to have a significant impact on the formation of massive stars [Larson, 2003].

During the initial collapse of a molecular cloud core to form a protostar, the dynamical timescale is crucial. It represents the timescale over which gravitational collapse occurs, leading to the formation of a protostar. Additionaly thermal timescale is relevant as the protostar heats up due to gravitational energy conversion. It represents the timescale over which thermal energy is redistributed within the protostar, regulating its internal temperature and pressure. On the other hand, in the earliest phases of protostar formation, nuclear processes have not yet begun so nuclear timescale is not to be mentioned. However, nuclear fusion reactions will eventually become relevant once the protostar reaches the main sequence phase [Pols, 2011].

1.1.3 Main Sequence Phase

When the protostar begins the process of nuclear fusion in its core, where hydrogen nuclei fuse together to form helium, it enters the main sequence (MS) phase. MS describes a specific region on the Hertzsprung-Russell diagram (H-R diagram), a tool for understanding the characteristics of stars, which is a graphical representation of the various stages and properties of stars (Figure 1.1. The main sequence is a diagonal band on the H-R diagram that represents the most common and stable stage of a star's life.

Stars spend the majority of their lives on the main sequence due to the abundance of hydrogen in the universe. The duration of this phase depends on the star's mass; more massive stars have shorter main-sequence lifetimes than less massive ones. During the main sequence phase, the dynamical timescale is relatively long compared to other timescales. It represents the timescale over which the star evolves due to gravitational interactions and changes in its structure. Thermal timescale remains important as the star continues to generate energy through nuclear fusion in its core. It represents the timescale over which energy generated by nuclear fusion is transported from the core to the surface, regulating the star's luminosity and

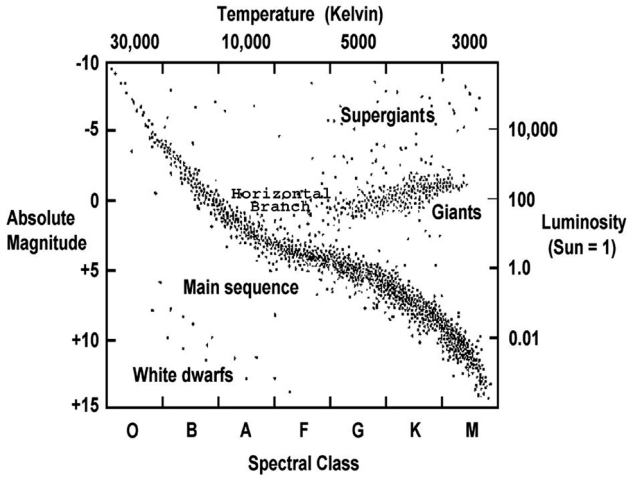

Figure 1.1: Hertzsprung-Russell diagram. In the vertical axes we have absolute magnitude and luminosity (in units of solar luminosity) on the left and the right respectively while on the horizontal axes the temperature (in Kelvin) on the top and spectral class on the bottom. Stars on the main sequence are located along a diagonal line from the top left (hot and luminous) to the bottom right (cool and less luminous) of the H-R diagram. Figure taken from [NASA, 2015].

stability. Furthermore, nuclear reactions in the core are the primary energy source for main sequence stars. The nuclear timescale represents the timescale over which hydrogen is converted into helium through fusion reactions, sustaining the star's luminosity and preventing further gravitational collapse [Pols, 2011].

As a main-sequence star exhausts its hydrogen fuel in its core, it will eventually leave the main sequence and enter a different phase of its life cycle, depending on its mass. This could involve expanding into a red giant, supergiant, or other processes.

1.1.4 Red-Giant Branch and Supergiants

As hydrogen in the core depletes, the star's core contracts and heats up, causing the outer layers to expand. For lower to intermediate-mass stars ($0.3 - 8\ M_{\odot}$), this leads to the formation of a **red giant**, while higher-mass stars ($from 8\ M_{\odot}$) become **supergiants***. Helium fusion occurs in the core during this phase, and creating heavier elements up to iron in the case of supergiants.

As the star evolves off the main sequence, the dynamical timescale may change due to changes in the star's structure and interactions with its environment, such as mass loss. The thermal timescale remains relevant as the star undergoes structural changes, such as expansion during the red giant phase or contraction during helium burning. Depending on the mass of the star, nuclear reactions may continue in shells surrounding the core, leading to the production of heavier elements and influencing the star's evolution and eventual fate, such as core collapse or planetary nebula ejection [Pols, 2011].

Red-Giant Branch (RGB) stars, typically characterized by their lower masses, often around 2 $M_{\odot}$. These stars progress through phases involving electron-degenerate helium cores and hydrogen-burning shells. During their evolution, they undergo the so called "first dredge-up," a process that involves the mixing of chemically processed material into the *convective envelope*. This results in changes in surface abundances of helium, carbon, and nitrogen. Simultaneously, the convective envelope extends further into the star, leading to a shift towards redder colors [Salaris et al., 2002].

When the helium core mass nears 0.5 solar masses, helium ignition occurs within the electron-degenerate core, generating a "He-flash." This flash lifts electron degeneracy and propels the star onto the Zero Age Horizontal Branch (ZAHB)**. Another specific feature in the evolutionary path of RGB stars is the "RGB bump." This bump signifies the star's reaction to a sudden surge in available fuel as the hydrogen-burning shell encounters a sharp discontinuity. This response causes a temporary drop in surface luminosity, followed by an increase as the hydrogen shell moves beyond the discontinuity. In the context of simple stellar

*Red giant and supergiant branches are also an H-R feature depicted in Figure 1.1

**The region on the Hertzsprung-Russell diagram where low-mass stars are located immediately after experiencing the helium flash.

populations, the positions on the Color-Magnitude Diagram (CMD),* and the expected number of stars during the red giant phase align closely with the RGB evolutionary track, especially for stars with similar mass and initial composition. RGB evolution transpires relatively swiftly, representing only a small fraction of a star's total lifespan [Salaris et al., 2002].

In essence, the evolution of RGB stars and aspects like their mass, chemical composition, mixing mechanisms, and core ignition are a few of crucial elements in understanding stellar populations and the broader field of stellar evolution.

Supergiants refers to the category of stars with an initial mass range of 8-12 solar masses. Following their departure from the main sequence, these massive stars undergo atmospheric expansion, becoming supergiants. However, stars with initial masses below 10 solar masses do not undergo iron core formation and thus do not enter the supergiant phase. Nevertheless, they can achieve luminosities thousands of times greater than that of the Sun. Ultimately, they shed their outer layers, leaving behind a white dwarf core [Massey and Olsen, 2003].

The massive supergiant stars (more than 10 $M_\odot$) deplete their hydrogen fuel, they smoothly transition to helium core fusion and proceed to fuse heavier elements until they form an iron core. At this crucial moment, the core's collapse cause the thermal energy due to fusion stops and the pressure from electron degeneracy can not match the gravitational pressure anymore and it triggers a Type II supernova event.

1.1.5 Stellar Afterlife

Stars continue to evolve, fusing heavier elements in their cores, including carbon, oxygen, and elements up to iron. This process is the reason for the creation of almost every element in the periodic table.

High-mass stars eventually undergo ***supernovae***, cataclysmic explosions that release an enormous amount of energy and can briefly outshine their host galaxies. The supernova is triggered from the collapse of the core and the remaining core can lead into a neutron star or a black hole. Lower-mass stars shed their outer layers more gently, forming a planetary nebula and leaving behind a white dwarf.

White dwarfs are the remnants of low-to intermediate-mass stars (mass up to 8 $M_\odot$) that have exhausted their nuclear fuel, mainly made up of electron-degenerate material. It is incredibly dense, with a mass similar to the Sun but a volume similar to the Earth. Masses typically range from about 0.1 to 1.4 times the mass of the Sun ($M_\odot$). The faint light emitted by a white dwarf is a result of the remaining heat energy it releases, as there is no nuclear fusion occurring within it. White dwarfs gradually cool over billions of years, becoming cold and dark objects known as black dwarfs.

A star with a mass in the range of 8 to 20 solar masses, has the potential to become a ***neutron star***. The mass of this compact object can range from around 1.4 to about 3 $M_\odot$. These extremely dense objects are formed from the collapsed cores of massive stars after a supernova explosion (see Subsection 1.1.7).

If the star is described by a mass greater than 20 $M_\odot$ then a ***black hole*** emerges from the death of the star after the supernovae explosion. Black holes represent the ultimate state of collapse, characterized by space-time singularities enveloped by event horizons.

It's important to note that the actual mass ranges of these compact objects can overlap and may vary based on theoretical models, observations, and additional factors, such as rotation and metallicity, that play a crucial role in the formation of these compact objects. Additionally, there might be other exotic or hypothetical compact objects not yet confirmed by observations, like primordial black holes or dark matter compact objects, that could fall into various mass ranges [Shapiro and Teukolsky, 2008].

For the purpose of this Thesis, the focus lies solely on neutron stars, quark stars, and their intermediary form, strange stars (see Subsection 1.1.9).

1.1.6 Stellar Wind

Stellar wind is an ongoing emission of charged particles, primarily electrons and protons, from the surface of a star into space. These winds originate from the outer layers of a star's atmosphere and exhibit variations in their speed and density, largely dependent on the star's size and temperature [Lamers and Cassinelli, 1999].

There have been three dominant theories on the originating of stellar winds [Cassinelli, 1979]. **Radiative models**, the primary theory, explain how stars, especially highly luminous ones, accelerate matter in their

*CMD is a graphical representation illustrating the correlation between the absolute magnitudes (brightness) of stars and their colors, which are intricately linked to their temperatures and spectral types.

outer atmospheres due to opacity near the energy peak. Early-type stars* achieve rapid acceleration from shifting ultraviolet lines into clear radiation fields, while late-type stars, with cooler atmospheres, drive dust and gas outward through radiative forces on infrared opacity, resulting in slower acceleration. On the other hand, **coronal models** suggest that stars with convection zones or other sources of acoustic and mechanical wave energy can develop coronal regions as a result of wave dissipation. This causes the outer atmosphere to expand into a wind, akin to the way the solar wind is generated. Furthermore, due to higher electron densities in stars, temperature structures in their outer atmospheres can differ from those in the expanding solar corona. Because the previews two models can not fully describe the stellar wind, there has been the idea of **hybrid models** which essentially combines radiative and coronal model.

The reason we mention stellar wind in this theoretical overview, is that we want to portray the main mechanism for mass loss in the single star evolution while in the binary evolution the mechanism depends mostly on the accreting material from on star to another (Section 1.3).

1.1.7 Neutron Stars: Formation Channels and Characteristics

The term neutron star was first suggested by James Chadwick and Walter Baade after the discovery of neutron in 1932 but it wasn't until the 1960s that we had the first observable proof (discovery of pulsars). Since then, neutron stars have been the subject of intense study due to the peculiar nature of this compact object [Carroll and Ostlie, 2017].

Neutron stars are incredibly dense objects that are formed when a massive star exhausts its fuel and undergoes a supernova explosion. During this process, the core of the star collapses under its own gravity, creating a highly compact object that is mostly composed of neutrons. Neutron stars have an extremely small radius of only 10-20 kilometers, yet they can have a mass of 1.4 to 2 times that of our Sun. This means that the density that describes them is extremely high, and the gravitational field they create is trillions of times stronger than that of the Earth [Shapiro and Teukolsky, 2008].

Due to their small size and high density, neutron stars have a unique set of physical properties that make them fascinating to study. For example, their intense gravitational fields can cause matter to be compressed to even more higher densities, allowing us to explore the behavior of matter under extreme pressure and temperature. Neutron stars are also known to have incredibly strong magnetic fields, which can generate intense radiation across the electromagnetic spectrum. In particular, they can emit beams of light and particles from their magnetic poles, creating a ***pulsar*** [Woosley et al., 2003], (see Section 1.1.8).

There has been a thorough research on the intricate mechanisms behind the formation of neutron stars, which has resulted in the identification of two distinct types of supernovae that play a vital role in their creation. The first type, known as iron-core collapse supernovae, occurs within massive stars nearing the end of their life cycles. These stellar objects develop a degenerate iron core that surpasses a critical mass threshold known as the *Chandrasekhar limit*. The core's immense mass triggers a catastrophic collapse, resulting in a huge explosion that propels the star's outer layers into space. While this cosmic chaos takes place, a neutron star emerges, pulsating with immense gravitational forces [Knigge et al., 2011].

In contrast, the second type, electron-capture supernovae, unfolds in lower-mass stars. Within these stars, hydrostatic equilibrium exists within an oxygen-neon-magnesium core. However, a dramatic event unfolds when electrons are abruptly captured by neon and/or magnesium nuclei. This disruption in equilibrium leads to the core's collapse, releasing a burst of energy. From this explosive climax, another neutron star is born, with its own unique characteristics shaped by the distinct nature of its birth [Knigge et al., 2011]. While the existence of these two types of supernovae has long been suggested, discerning the specific families of neutron stars resulting from each channel has proven challenging. However, a breakthrough study has unveiled an unexpected connection within a well-known class of neutron-star-hosting X-ray pulsars called Be/X-ray binaries [Reig, 2011].

These celestial objects consist of neutron stars that accrete matter from more massive companion stars. Astonishingly, this group has been found to harbor two distinct sub-populations with divergent attributes. These sub-populations exhibit contrasting spin periods, orbital periods, and orbital eccentricities, suggesting a strong correlation with the two types of supernovae. Further analysis reveals that neutron stars born from electron-capture supernovae tend to possess shorter spin periods, shorter orbital periods, and lower eccentricities. In contrast, those arising from iron-core collapse supernovae exhibit different properties, indicative of their unique formation process.

*Early type stars, is usually a term referring to stars with higher temperature, while late type referring to the stars with lower temperature

It's important to note that these types of supernovae are believed to be responsible for the majority of neutron stars in the universe, but there may be other formation channels as well.

Equations of state

The equation of state (EoS) is a fundamental principle in physics that defines the connection between a system's macroscopic properties, like pressure, temperature, density, and energy, given specific conditions. In the case of compact objects such as white dwarfs and neutron stars, the EoS sheds light on how matter behaves when subjected to intense pressure and density [Lattimer and Prakash, 2007].

For instance, the EoS for neutron stars indicates how pressure and density interrelate as matter becomes highly compressed in the core. This equation is pivotal for comprehending the inner structure, stability, and observable characteristics of these kind of stars. The general formula for an equation of state for an ideal gas can be represented as follows:

$$P = P(n, T) \ , \tag{1.1.5}$$

where P stands for the system's pressure, n denotes the system's density and T signifies the system's temperature (which may be pertinent in certain scenarios). In the case of a degenerate gas the pressure behaves as follows:

$$P = \frac{(3\pi^2)^{2/3} h^2}{5m} \left(\frac{N}{V}\right)^{5/3} \ , \tag{1.1.6}$$

where h is Plank's constant, N is the number of particles, V is the volume and m is the mass of a single particle. When the density is extremely higher and the matter returns to quantum state the pressure can be described with the following proportional

$$P \propto \left(\frac{N}{V}\right)^{4/3} \tag{1.1.7}$$

thus, temperature is not the main factor that affects pressure in the degenerate gas case.

As neutron star matter is primarily degenerate, the EoS remains mostly unaltered by fluctuations in temperature. In this context, the matter's characteristics are primarily governed by quantum mechanical effects, causing temperature to have limited influence on properties such as density and pressure. So we need a function of P that is only depending on the density n of the neutron star, P(n). The specific formulation of the equation of state hinges on the nature of the material within the system. Concerning neutron stars, the equation of state involves intricate interactions among neutrons, protons, electrons, and other particles.

Various density ranges exhibit distinct physical behaviors and material phases. When matter enters a density range characterized by a different equation of state, it might cause a ***phase transition*** from baryonic (protons, neutrons) matter to quark matter (up and down quarks). The understanding of dense matter is well-established and validated up to nuclear density ($n_{\text{nuc}} = 0.16\ \text{fm}^{-3}$), but in the cores of neutron stars, which often surpass this extreme density, the reliability of physical theories diminishes significantly [Shapiro and Teukolsky, 2008].

To conclude, EoS will be the key to the problem of understanding the neutron star's structure and consequently its properties that play crucial role in its evolution and shall give us insights about the relationship between some important quantities, such as mass and radius, of the star, which might explain some peculiar behaviors of the eccentric millisecond pulsars, (see Chapter 2).

1.1.8 Pulsars

In the previous Section, it was suggested that pulsars exhibit a close association with neutron stars. Even though Anthony Hewish and Jocelyn Bell Burnell discovered the first pulsar, PSR B1919+21, in 1967 they did not know what was these "pulses". Pulsars initially baffled astronomers due to their pulse-like signals, which resembled clock-like precision and led to speculation about extraterrestrial intelligence. Their rapid periodicity challenged understanding of how compact objects could rotate so swiftly without disintegrating. Furthermore, their stable pulse periods over time suggested an extraordinary source of stability, defying existing astrophysical models. Pulsar signals also exhibited highly regular dispersion measures, indicating a consistent delay in arrival times across radio frequencies. Adding to the mystery, pulsars lacked visible light emission, deviating from the behavior of typical celestial objects [Cordes et al., 2004]. Thus, the observations concerning their mass, radius, and spin period where lacking the proper understanding and the mystery of the essence of pulsars needed to be determined.

There were a few possible explanations about what was the true nature of pulsars. Initially it was hypothesized that it might be **binary star systems** and that we observe the luminosity change due to the rotation of the stars as the "pulse". But this is not the case according to Einstein theory of relativity as the gravitational waves of the stars would transfer energy outside of the system and due to the spiral orbit that exist, the period is being reduced, according to Kepler's third law. Another scenario was that pulsars where **pulsating stars**, also known as variable stars. These are stars that undergo regular changes in their brightness over time. These changes in brightness are caused by the expansion and contraction of the star's outer layers, which in turn affect its luminosity. Pulsations can occur due to various physical processes happening within the star. Unfortunately these pulsations last for a few seconds which is way longer than the pulse that was detected. An alternative proposition was that that pulsars are **rotating stars** but the problem now is what is the maximum speed that these stars can achieve. Normal stars have limits to the minimum spin period P_{min} depending on their radius R and mass M according to equation:

$$P_{\text{min}} = 2\pi\sqrt{\frac{R^3}{GM}}\ , \tag{1.1.8}$$

where G is the gravitational constant equals.

So for normal stars we have a minimum spin period of a few seconds which still dose not fit our problem. However if the rotating star is a **neutron star** then the observations and theory match as some pulsars where detected as the remnants of a supernovae [Carroll and Ostlie, 2017]. To conclude, a pulsar is a type of neutron star that spins rapidly and has a strong magnetic field. It emits beams of electromagnetic radiation from its magnetic poles, which can be seen as pulses when they face Earth. Pulsars have compact cores and predictable rotation periods, leading to precise intervals between pulses.

The $\dot{P} - P$ diagram

The $\dot{P} - P$ diagram is a graphical representation used in pulsar astronomy. This diagram plots the rotational period (P) of pulsars against their period derivative ($\dot{P}$), which is a measure of how the period is changing over time. The $\dot{P} - P$ diagram is instrumental in studying the evolutionary paths of pulsars. It helps classify pulsars into distinct regions, providing insights into their ages, magnetic field strengths, and other important properties. Different regions on the diagram correspond to different evolutionary stages in the life cycle of pulsars [Phinney and Blandford, 1981].

The pulsar death line is a boundary in the $\dot{P} - P$ diagram that separates radio-loud pulsars from radio-quiet sources. Traditionally, radio-loud pulsars are expected to be above this line. However, advancements in observation equipment have revealed diverse properties of neutron stars. Some special sources are radio-quiet but still lie above the death line, indicating that different equations of state for neutron stars result in different death lines. Understanding the equation of state's influence on the death line and the connections between different neutron star groups is important. Central compact objects may be small, self-bound strange stars, while rotating radio transients could be old pulsars nearing the end of their active phase [Zhou et al., 2017].

The $\dot{P} - P$ diagram is also an extremely useful tool for good estimations about the magnetic field B, the characteristic age τ_c and the the energy lose $\dot{E}$ as we can see in Figure 1.2. More specifically:

(i) **Magnetic Field Strength (B)**: The strength of a pulsar's magnetic field at its surface is directly related to the square root of the product of its period and the rate of change of that period, meaning pulsars with different P and $\dot{P}$ values will exhibit notably distinct magnetic field strengths.

$$B_{\text{p}} = \frac{1}{sin\alpha}\left(\frac{3Ic^3P\dot{P}}{2\pi^2R^6}\right)^{1/2}\ , \tag{1.1.9}$$

where α is the inclination angle, I is the moment of inertia, c is the speed of light, and R is the radius of a pulsar.

(ii) **Characteristic Age (τ_c)**: It represents a pulsar's estimated age based on its current rotational properties and is calculated as $\tau_c = P/(2\dot{P})$.

(iii) **Spin-Down Luminosity ($\dot{E}$)**: The rate at which a pulsar loses its kinetic energy, termed the spin-down luminosity, is inversely proportional to the cube of its rotational period and directly proportional to its rate of period change. Mathematically, $\dot{E} \propto \dot{P}/P^3$ [Lorimer, 2008].

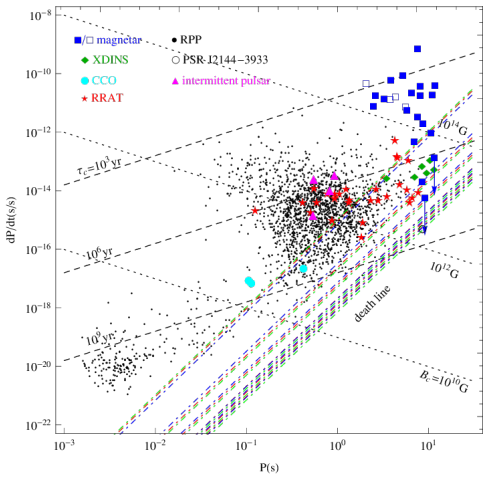

Figure 1.2: The $P - \dot{P}$ diagram. Objects represented by blue squares are magnetars. Empty squares within this group indicate radio-loud magnetars. Green diamonds on the figure represent X-ray dim isolated neutron stars (XDINSs). Circular markers in cyan designate central compact objects (CCOs). Objects shown as red stars correspond to rotating radio transients (RRATs). Magenta triangles on the figure symbolize intermittent pulsars. Objects represented by black dots are rotation-powered pulsars. This category includes both normal pulsars and millisecond pulsars, which make up the majority of the pulsar population. Black open circles denote PSR J2144−3933. Picture taken from [Zhou et al., 2017]

Also from the $P - \dot{P}$ diagram we can come to some logical conclusions about pulsars and their properties, as [Ohse, 2021] noted:

- **Luminous Pulsars**:Typically, pulsars exhibiting the highest luminosity are in their youthful stage. These pulsars have extended rotational periods, and undergo rapid slowing down in their rotation.
- **Magnetic Field Consistency**: When pulsars experience a spin-down process the $\dot{P}$ follows the following power law:
$$\dot{P} \propto P^{2-n} \tag{1.1.10}$$
where index n is approximately 3 ($n \simeq 3$), and their magnetic field strength remains relatively steady.
- **"Graveyard" Phase**: Within a region commonly denoted as the "graveyard," characterized by an energy loss rate ($\dot{E}$) dropping below 10^{30} erg/s, there is a notable reduction in the population of pulsars.
- **Divergent Pulsar Sub-Groups**: Subcategories of pulsars, like long-period ones and millisecond pulsars, exhibit substantial distinctions in their characteristics.
- **Millisecond Pulsars**: Millisecond pulsars (MPs) are recognized for their remarkably stable rotation and relatively modest magnetic fields, usually around 10^8 Gauss (G), (see Subsection 1.2.4).

1.1.9 Strange stars

Neutron stars, as mentioned before, exhibit subdivisions based on their dominant phases and equations of state. Ordinary neutron stars consist exclusively of hadronic matter, featuring an extensive crystalline crust. Hybrid stars possess a dynamic composition, comprising a liquid quark core, a surrounding hadronic shell, and a solid crust. Theoretical in nature, strange stars propose the existence of macroscopic up, down, and strange quark matter objects, potentially lacking a discernible crust. Understanding the formation, properties and structure of neutron stars is intricately linked to the development of their equation of state [Alcock et al., 1986], (see Section 1.1.7). However, constructing plausible equation of state remains an ongoing pursuit, integrating theoretical models and observational data to refine our understanding. While ordinary neutron stars are widely acknowledged, further investigation is needed to establish the existence and properties of hybrid stars and strange stars.

1.2 Evolution of Binary Star Systems

The evolution of close binary stars follows a distinct path compared to single stars. Single stars can often be approximated as spherical and described using relatively stable models during most phases. In contrast, close binary stars, which interact through mass exchange at some point in their journey, introduce a more complex three-dimensional scenario. Tidal forces in these systems can result in departures from spherical symmetry, leading to rapid rotation in one or both stars. Tidal heating becomes a significant factor. When mass transfer occurs, various physical processes like turbulent viscosity and meteorological phenomena come into play, although they lack well-defined quantitative descriptions [Iben Jr, 1991].

Close binary star evolution doesn't readily yield precise, mathematically rigorous models for direct comparisons with observations. Instead, the field relies on a collection of general concepts, guidelines, and algorithms to construct qualitative scenarios that outline how close binary systems progress through various interaction phases. Observational paradigms, which are systems clearly impacted by intense interactions in the past or destined for such interactions in the future, play a crucial role in this context. These paradigms help maintain consistency with the constructed scenarios, although occasional adjustments are needed to align principles and algorithms with observed properties. Close binary star evolution necessitates a blend of qualitative and quantitative approaches to gain a comprehensive understanding.

In this section we are going to discuss how a binary star system behaves as time passes and what differs from the single star evolution.

1.2.1 Binary Vs Single Star Evolution

In the case of binary star evolution its instinctively true to think that there are some key differences in comparison to the single star evolution. The following paragraphs note the most important differences.

When there is a system of objects with mass, there is a *gravitational interaction*. Each star exerts a gravitational force on the other, which keeps them in orbit. The strength of this force depends on the mass of the stars and the distance between them, following Newton's law of universal gravitation. The gravitational interaction between the two stars can lead to changes in their orbital parameters, such as eccentricity and separation. This can affect the binary system's long-term stability and eventual fate. As they orbit, the stars constantly feel the gravitational pull of each other, which results in their *orbital motion*.

The interaction due to orbital motion of the stars also is an important distinction. Stars revolve around their common center of mass in elliptical orbits. The shape and size of these orbits depend on the masses of the stars and their separation. Size of the orbits in a binary system is influenced by the combined mass.

Tidal forces are a consequence of the varying gravitational pull of one star on the other as they move through their elliptical orbits. These tidal forces can lead to the deformation of the stars, causing them to become slightly elongated in the direction of the companion star. Tidal interactions can also lead to the transfer of angular momentum between the stars, causing changes in their orbits and consequently in their evolution [Hut, 1981]. Additionally, tidal forces is the reason that binaries after a period of time $\sim 10^4$ years obtain a circular orbit.

In some binary systems, when one star evolves and expands, it may devour its companion in a *common envelope*. This shared envelope of gas can cause the two stars to spiral inward, leading to a close binary system or even a merger of the two stars. This process can result in the formation of various exotic objects like cataclysmic variables, X-ray binaries, or even binary black hole systems [Paczynski, 1976]. Furthermore, in some binaries, one star can transfer mass onto its companion. This typically occurs when one star expands and becomes a giant or supergiant, and the other star is close enough to capture some of the material from its outer layers. This process can lead to the formation of accretion disks and the transfer of matter between the stars (see Subsection 1.2.2).

The presence of a companion star can alter the rate at which a star evolves. Mass transfer, for instance, can change the mass and composition of a star, leading to different evolutionary tracks in the Hertzsprung-Russell diagram. Binary stars can experience enhanced *mass loss* through processes like Roche-lobe overflow or stellar winds, which can deplete the stars of their outer layers and affect their chemical composition. Binary interactions can influence the outcome of stellar evolution, potentially leading to different types of supernovae and the formation of various compact objects, such as white dwarfs, neutron stars, and black holes.

1.2.2 Roche-Lobe

The Roche lobe (RL) is a theoretical concept applied in binary star systems. It defines a region where one star's gravitational influence prevails over the other, determining the orbits of the stars and affecting how they exchange mass. In simpler terms, two stars in a close binary system, are attracted to each other by gravity. Each star exerts its gravitational force. The Roche lobe represents an area around each star where its gravitational pull is stronger than that of its companion [Postnov and Yungelson, 2014].

Understanding the Roche lobe is crucial when stars in a binary system transfer mass via accretion process. If a star expands beyond its Roche lobe, it can transfer mass to the other star, typically through a process known as ***Roche-lobe overflow***. This phenomena leads to various astronomical events, including the formation of accretion disks, X-ray binaries, and cataclysmic variables. In order to explain this phenomenon, a better understanding of the dynamics of the system, also known as the Roche-lobe potential, is required.

The Roche-lobe potential is the gravitational energy environment within a binary star system, particularly near the Roche lobes. These lobes represent regions around each star where its gravitational force dominates over its companion's. Figure 1.3 provideσ a better understanding of this concept.

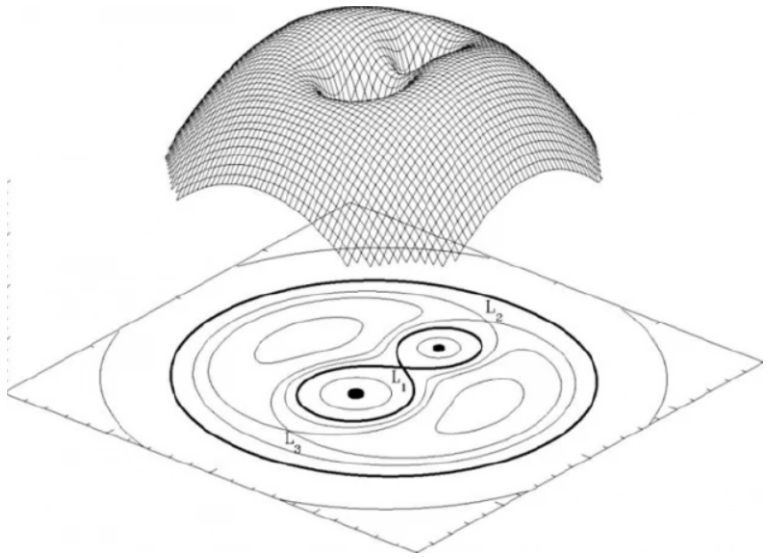

Figure 1.3: Roche-Lobe potential. A visual representation in three dimensions of the Roche potential within a co-rotating frame, specifically designed for a binary system with the ratio of donor mass to the mass of the compact star equal to two. L_1, L_2 *and* L_3 are the 3 Lagrangian points. Figure taken from [Postnov and Yungelson, 2014].

Roche-Lobe Overflow

Roche-lobe overflow (RLOF) occurs in binary star systems when one of the stars fills its lobe and expands beyond its gravitational boundary, the Roche lobe. This can happen through various stellar processes (such as entering the red giant or supergiant phase), leading to material transfer from the star that exceeds its RL boundary to the primary star (neutron star), through L_1 and forming accretion disks, profoundly influencing the binary system's evolution [Hilditch, 2001].

The Roche-lobe radius, also known as the Roche limit, is a critical distance within which the gravitational forces between two celestial bodies, such as a star and a planet or two stars in a binary system, become significant. It depends on the masses and separations of the two objects in question. The basic formula to calculate the Roche-lobe radius (R_{L}) for a binary star system is [Eggleton, 1983]:

$$R_L = r\frac{0.49q^{2/3}}{0.6q^{2/3} + ln(1 + q^{1/3})} \ , \tag{1.2.1}$$

where r is the separation radius and q is the ratio of the donor mass to the mass of the neutron star. This formula provides an approximation of the Roche lobe radius for a binary system. In practice, it can be more complex, especially when dealing with eccentric orbits or non-spherical objects but for this project this is will not be an issue. In the case of R_{L} and R_{don} evolve and expand with the same rate, the RLOF is a stable process and we can set a parameter for the stability of the mass transfer. First we need to define

a relation between the two radius and the donor's mass. According to [Tauris and Van Den Heuvel, 2006] they are proportional with the following power-law relation $R_i \propto M_{don}^{\zeta_i}$, where ζ_i*:

$$\zeta_{don} = \frac{\partial lnR_{don}}{\partial lnM_{don}},\ \zeta_L = \frac{\partial lnR_L}{\partial lnM_{don}} \tag{1.2.2}$$

So the initial stability is regulated by the ζ_* factors and so as to be the overflow stable at the starting point, the two factors should satisfy this condition:

$$\zeta_{don} \geq \zeta_L \tag{1.2.3}$$

At some point ***Roche-Lobe Decoupling Phase*** (RLDP) accrues. This phase occurs when the stars in the binary system become detached from their respective Roche lobes due to changes in their sizes, masses, or orbital parameters. This can happen for various reasons, such as mass transfer between the stars, stellar winds, or changes in the stars' internal structure. The RLDP involves a decrease in mass transfer rate, and in the case of MSPs, causing the pulsar's magnetosphere to expand and exert a braking torque, leading to an increase in its spin period. As RLDP progresses, the spin equilibrium is eventually broken, with the magnetosphere expanding faster than the spin can adapt, resulting in a shorter spin period. Also in this phase, the accretion process is not as efficient [Tauris, 2012].

Roche-Lobe Overflow Cases

In close binary star systems, mass transfer from one star to another occurs in different scenarios based on the evolutionary stage of the donor star [Savonije, 1978]:

Case A: Mass transfer starts when the donor star is undergoing central hydrogen burning, usually before it reaches the terminal-age main sequence.

Case B: Mass transfer initiates when the donor star transitions from the main sequence to the terminal-age main sequence, just before helium ignition occurs.

Case C: Mass transfer begins during helium shell burning or even later phases of stellar evolution [Tauris and Van Den Heuvel, 2006].

Mass transfer rate

To initiate mass transfer in a binary star system, one of the stars must exceed its Roche lobe's boundaries and maintain this condition. This can be achieved through two fundamentally different processes according to [Podsiadlowski, 2014]:

In the first scenario, the donor star attempts to expand due to its internal evolution. This expansion can take place gradually over an extended period, known as a nuclear timescale, or more rapidly on a shorter thermal timescale. The second scenario involves the binary system losing angular momentum, resulting in a contraction of the orbital distance between the stars. As a consequence, one of the stars overshoots its Roche lobe boundary. We can assume that the magnitude scale of the mass transfer rate follows:

$$\dot{M} \sim \frac{M_{don}}{\tau_{nuc}} \tag{1.2.4}$$

when the expansion of a star is the result of nuclear evolution.

1.2.3 Accretion process

Accretion is a process that involves the accumulation of material onto a central object due to gravitational forces. This process is observed not only in low-mass X-ray binaries (see Section 1.2.5) and is playing a very important role in celestial body formation and evolution. It begins with gravitational attraction, drawing material towards a central object, often forming a rotating accretion disk. Material within this disk moves inward due to angular momentum transfer, releasing energy in the form of radiation. The rate of material accumulation varies widely [Pringle, 1981].

Accretion is observed in star formation, black hole growth, planetary ring formation, and celestial object behavior. Accretion disks, common in this process, exhibit complex dynamics and emit intense radiation, observable in multiple wavelengths.

*i is placed as an index for the "values" *don* and *L* respectively

1.2.4 Millisecond Pulsars

Millisecond pulsars are a type of neutron star that rotate rapidly and emit regular pulses of electromagnetic radiation, usually in the form of radio waves. They have rotational periods that range from a few milliseconds to tens of milliseconds, which is much faster than typical pulsars [Nurmamat et al., 2019]. The typical radius for that kind of pulsar is 20-30 km. These pulsars are believed to be old neutron stars that have been spun up by accreting material from a companion star in a binary system. The accretion process causes the neutron star to spin faster and faster, until it reaches its current fast rotation rate.

Millisecond pulsars are important objects for a variety of astrophysical studies. They are used as precision clocks for tests of general relativity and the properties of the interstellar medium. They can also be used to study the evolution of binary star systems and the formation and dynamics of globular clusters. Additionally, millisecond pulsars are important sources of gravitational waves and are potential targets for future space-based gravitational wave detectors.

Most millisecond pulsars can be found in a binary system or if they were spotted alone the most common theory is that the MSPs basically evaporated their companion through years of devouring their accreting mass.

If we get in more detail, the process that characterizes this system begins with material transfer from the companion star onto the neutron star. This inflowing matter, as it falls onto the neutron star's surface, transfers angular momentum, significantly increasing the neutron star's rate of rotation. This phenomena, termed ***"recycling,"*** turns the initially slow-rotating neutron star into a high-speed MSP [Tauris and van den Heuvel, 2023].

Over time, MSPs can lose their companion stars through various processes (accretion, tidal forces). Once isolated, they continue to emit stable pulses, albeit slowing down gradually over billions of years.

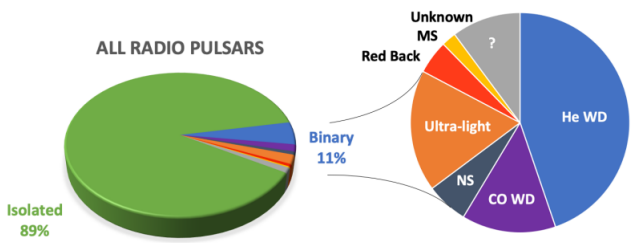

Figure 1.4: Categories of radio pulsars. The pie chart on the left panel shows every category of radio pulsars and on the right panel shows the categories of binary systems that the pulsar belongs in retrospect with the summation of all the radio pulsars in the visible universe. Figure taken from[Tauris and van den Heuvel, 2023].

Eccentric Millisecond Pulsars

Eccentric millisecond pulsars (EMSPs) are a subclass of neutron stars that exhibit eccentric (non-circular) orbits around their binary companions. The eccentricity in their orbits means that their distance from the companion star varies during the orbit. The majority of observed EMSPs have an eccentricity of ~ 0.1 and an orbital period in the range of 20-50 days.

The odd thing about eccentric MSPs that has divided the astrophysicists is that after a period of time around 10^4 years, due to tidal forces, in the low mass binary system the orbit should have been circular. However the results of a great number of observations state the existence of these peculiar objects. As a result there has been a few new hypotheses on the formation of the EMSPS.

In 2013 Frerie and Tauris suggested that eccentric binary millisecond pulsars may form differently than previously thought [Freire and Tauris, 2013]. Instead of gradual spin-up via accretion in circular orbits, these MSPs could directly originate from collapsing super-Chandrasekhar mass white dwarfs. On the other hand, in 2014 Antoniadis proposed that the significant increase in eccentricity observed in these systems may result from the dynamic interaction between the binary system and a surrounding circumbinary disk

[Antoniadis, 2014]. This disk could form from material ejected during hydrogen flash events when the neutron star is already an active radio pulsar and tidal forces can no longer circularize the binary. Last but not least, in 2019 Alvarez-Castillo and others, through numerical calculations, recommended the potential for neutron stars to undergo a sudden change in their nature, shifting from being entirely made of hadronic matter to becoming stable hybrid stars on a third-family branch, with a transitional phase of instability in between [Alvarez-Castillo et al., 2019].

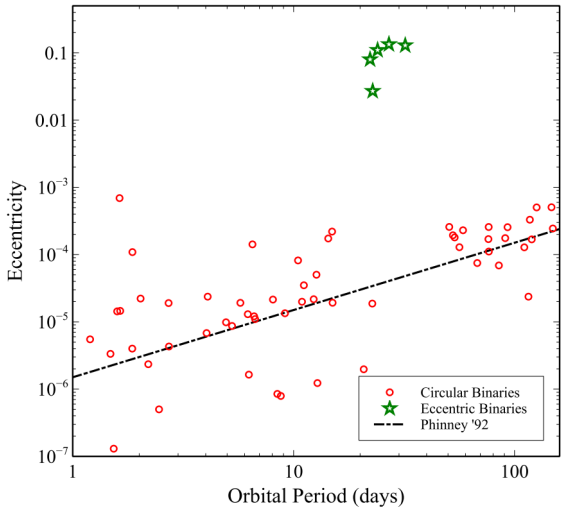

Figure 1.5: Eccentricity vs orbital period for millisecond pulsars with a white dwarf as their companion. In 1992 Phinney theorized (fluctuation-dissipation theorem) that all binaries should follow a linear relation in the above diagram (dashed line) [Phinney, 1992]. However, even though circular binaries (shown here as circular mark, ○) satisfy this relation, eccentric binaries (depicted with a star mark, ⋆) diverge. The EMSPs have an an eccentricity of ~ 0.1 and an orbital period in the range of 20-50 days. Figure taken from [Antoniadis et al., 2016].

Formation of Millisecond Pulsars

Initially, a binary system forms with two stars with masses in the range of 1-2 $M_\odot$ and 10-15 $M_\odot$, one of which is destined to become a white dwarf, while the other will eventually become a neutron star. Both stars evolve from a Zero-Age Main Sequence (ZAMS) phase. The more massive of the two evolves faster and eventually exhausts its nuclear fuel, expanding into a red giant. This process can lead to RLOF and eventually to mass transfer between the two stars.

As the red giant expands, it can transfer material onto its companion. If enough mass is transferred, it can lead to the formation of an accretion disk around the neutron star, resulting in the emission of X-rays and other radiation [Hilditch, 2001]. The more massive star eventually goes supernova, resulting in the formation of a ***neutron star***. If the neutron star receives mass from its companion through accretion process, it can spin up and become a rapidly rotating neutron star or ***MSP***. The less massive star will eventually burn all the hydrogen in its core and move on to the red giant phase. From this point on due to the expansion of the star, the Roche-lobe will be filled and the red giant will transfer mass through L_1 (RLOF) leading to a low-mass X-ray binary system. At some point the red giant will evolve into a ***white dwarf***. The MSP-WD system can remain stable, where the white dwarf continues to lose mass through various mechanisms, such as stellar wind or Roche-lobe overflow, sustaining the MSP's activity.

The evolution of low-mass binary systems into neutron star-white dwarf systems and the subsequent transformation into MSPs is a process that involves a combination of stellar evolution, mass transfer, and the intricate physics of compact objects. [Tauris and van den Heuvel, 2023] give us a better understanding of the hole process and in Figure 1.6 we see step by step the main parts of the evolution of this type of binary.

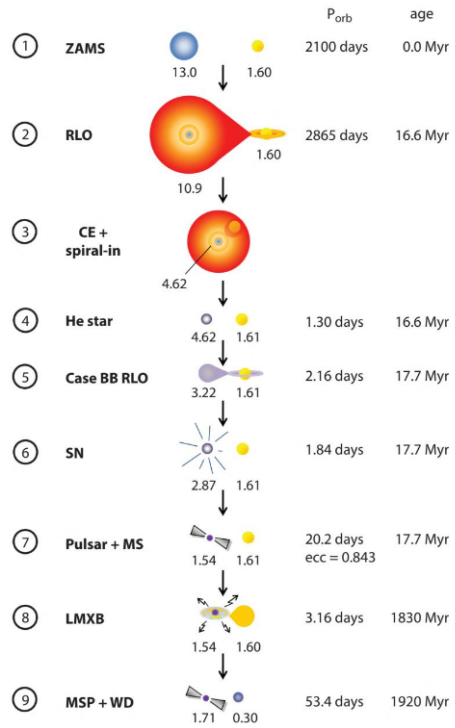

Figure 1.6: Evolution of a binary to a NS-WD system. A simple visualization of the different stages of evolution of a binary system that in the final stage becomes a MSP-White Dwarf system. The initial masses are 10-15 $M_\odot$ and 1.0-2.0 $M_\odot$ respectively. Figure taken from [Tauris and van den Heuvel, 2023].

1.2.5 X-Ray Binary Systems

X-ray binaries are objects in our universe, composed of a normal star and a compact object in orbit around each other. The compact object can be a white dwarf, neutron star, or black hole, and its strong gravitational field attracts material from the normal star [Lochner et al., 2004]. As this material falls towards the compact object, it is heated to incredibly high temperatures, up to millions of degrees, and emits X-rays that can be detected by X-ray telescopes. These binaries are dynamic systems that undergo a variety of phenomena, including outbursts, eclipses, and variability in X-ray emission. These phenomena provide important clues to the physical processes that are happening in these systems. Some X-ray binaries go through periodic outbursts that can last from days to years, during which the X-ray emission from the system can increase by several orders of magnitude, which can be attributed to the enhanced accretion of material onto the compact object. Studying these outbursts can help us understand the accretion processes that drive X-ray emission, as well as the dynamics of the material in the binary system [Schatz and Rehm, 2006].

Accretion in X-ray Binaries

Accretion in X-ray binaries depends on the companion star's characteristics and as a result we have two different categories [Miskovicova, 2021]:

a) **Low-Mass X-Ray Binaries (LMXB)**: In these systems with low-mass companions, a stream of material enters through the first Lagrange point. High angular momentum prevents direct infall onto the compact object, leading to the formation of a large accretion disk. Viscosity-induced friction in the disk heats the gas, causing energy radiation, and gradual sinking into the compact object's gravitational well.

b) **High-Mass X-Ray Binaries (HMXB)**: HMXBs feature massive companion stars with strong stellar winds. These winds, shaped by the compact object's gravity, focus a portion onto the compact object. This accretion process results in smaller accretion disks but maintains a high mass accretion rate, generating intense X-ray emissions.

1.3 Phase Transition

A phase transition is a process denotes a shift in the state of matter within a system due to alterations in external factors like temperature, pressure, or composition. This transformation typically involves transitions between common phases of matter such as solid, liquid, and gas [Onuki, 2002]. In the case of neutron stars, phase transition occurs when baryonic matter undergoes intense heat and pressure, such as that within neutron stars. During this extreme conditions the protons and neutrons of the neutron star might disassemble. This disintegration would release the quarks and gluons contained within and essentially baryonic matter will transform into quark matter. This phase transition in matter can lead to a dynamical asymmetric kick that would cause a binary system, for example, to change its orbital reconfiguration.

Mass loss

During the phase transition process, the gravitational mass, which represents the sum of baryonic mass and the binding energy, is reduced [Gao et al., 2020]. On the other hand, the baryonic mass is preserved. So we can conclude that the loss of mass is associated with the differentiation of the binding energy. With the use of Einstein's formula for mass-energy relation we can calculate the mass loss:

$$E_{\Delta} = \Delta M c^2 \ , \tag{1.3.1}$$

where ΔM is the mass loss and c is the speed of light.

1.3.1 Kick Mechanism and Orbit

Before we start this subsection, we need to be sure that the transition can cause a kick to disrupt the equilibrium of the circular orbit.

$$\tau_{\rm ff} = \sqrt{\frac{R_{\rm ns}^3}{GM_{\rm ns}}} \simeq 0.1 \text{ ms} \tag{1.3.2}$$

The free-fall timescale of a neutron star is always smaller than its spin period or orbital period.

In 2006, Berdermann, studied a model that explains gamma-ray bursts and star kicks by directing neutrino emissions along magnetic vortex lines. With initial temperatures between $30-60\ MeV$ and surface magnetic fields from $10^{15} - 10^{17}\ G$, it releases significant energy within a narrow beam (up to $10^{52}\ erg$), depending on the magnetic field's strength [Berdermann et al., 2006]. This mechanism, combined with the influence of magnetic fields on neutrino-producing weak interactions, can produce star kicks with velocities similar to observed pulsar kicks. For that reason the mechanics is the same, thus one can treat the phase transition kick as a supernovae kick. So the equations that describe the orbit, in accordance with [Hills, 1983] and [Tauris and Van Den Heuvel, 2006] will be presented and discussed for further understanding. We assume that the orbit before the transition is circular which means $e = 0$, and that the relative velocity of the two stars in this circular system is given by the following equation:

$$u_{\rm rel} = \sqrt{GM/r},\ \ M = M_{\rm don} + M_{\rm ns} \ , \tag{1.3.3}$$

where M is the total gravitational mass as portrayed above. The post-transition semi-major axis ($a_{\rm pt}$*) can be described as follows:

$$\frac{a_{\rm pt}}{r} = \frac{1 - \Delta M/M}{1 - 2\Delta M/M - (w/u_{\rm rel})^2 - 2cos\theta(w/u_{\rm rel})} \ , \tag{1.3.4}$$

where r is the pre-transition semi-major axis, ΔM is the amount of mass lost in the phase transition, w is the magnitude of the kick velocity, and θ is the direction of the kick relative to the orientation of the pre-transition velocity.

The kick magnitude can determine the nature of the collapse. In the case of $w = 0$, we have an *isotropic* collapse while for $w \neq 0$ the *asymmetric kick* occurs. In the second case, we shall mention that a percentage of the energy, that is channeled, is turned to kinetic energy for the neutron star. When the magnetic field channels all high-energy neutrinos in a specific direction, it aligns the released energy with relativistic kinetic energy and we can attain the maximum kick velocity $w_{\rm max}$ as follows:

*We use the "pt" notation to be able to distinguish the post-transition quantities

$$E_\Delta = E_K = \frac{M_{\rm ns}^{\rm pt} c^2}{\sqrt{1-(w/c)^2}} - M_{\rm ns}^{\rm pt} c^2 \Rightarrow w_{\rm max} = c\sqrt{1 - \frac{(M_{\rm ns}^{\rm pt})^2}{(M_{\rm ns}^{\rm pt} - \Delta M)^2}} \ . \tag{1.3.5}$$

Now we need to check if the kick will disrupt the binary equilibrium and change the orbit. For that reason we compute some values for the w_{max} based on the mass of the pulsar for a range of 1.46-1.65 $M_\odot$. After some simple calculations we have a range of $\sim 30000 - 60000\ km/s$ for the maximum velocity kick. Because the pre-trantision relative velocity of the neutron star has a value of $u_{rel} \sim 100\ km/s$ the isotropic kick is unable to disrupt the system, while the asymmetric one can change the orbit of the binary.

Besides the order of the magnitude, we need to define the orientation in a 3-D space, so we introduce the angle (ϕ) between the kick velocity ($\vec{w}$) and the vector ($\vec{r}$) of the pre-transition orbital plane. We are now able to attain a formula for the post-transition eccentricity:

$$e_{pt} = \sqrt{1 - \left(\frac{r}{a_{pt}}\right)^2 \frac{(u_{rel} + wcos\theta)^2 + (wsin\theta sin\phi)^2}{(u_{rel}^{pt})^2}} \ , \tag{1.3.6}$$

while the post-transition relative velocity

$$u_{rel}^{pt} = \sqrt{GM_{pt}/a_{pt}} \ . \tag{1.3.7}$$

After the phase transition process and the disruption of the binary, if the system has not been wiped out or collapsed, the post-transition period is essentially a Keplerian period:

$$P_{orb}^{pt} = 2\pi\sqrt{\frac{a_{pt}^3}{GM_{pt}}} \ . \tag{1.3.8}$$

If we want the most effective kick orientation, it must be parallel to the angular momentum of the neutron star (J_{ns}) and inductively to the angular momentum of the orbit. So the values for the angles in a "perfect" kick should be $\theta = \phi = \pi/2$ which simplifies the equations 1.3.4 & 1.3.6 as follows:

$$\frac{a_{pt}}{r} = \frac{1 - \Delta M/M}{1 - 2\Delta M/M - (w/u_{rel})^2} \quad \& \quad e_{pt} = \sqrt{1 - \left(\frac{r}{a_{pt}}\right)^2 \frac{(u_{rel})^2 + (w)^2}{(u_{rel}^{pt})^2}} \ . \tag{1.3.9}$$

1.4 Thesis Outline

In this section we will give a brief explanation on the purpose of this thesis and connect the essential theory, to the actual work and calculations.

Essentially there is a need to explain the orbit of a binary system, that consist of a millisecond pulsar as the primary star and a white dwarf as the companion star, is elliptical and not circular, through the process of phase transition in matter, thus creating an eccentric millisecond pulsar. As mentioned before, at the end of its evolution, the binary should have a circular orbit but observations have stated otherwise for the eccentric MSPs [Antoniadis et al., 2016]. Although if we consider that phase transition occurs, then the asymmetric kick will set the system in an elliptic orbit. Before we embark on examining the phase transition conditions and their alignment with observations, it is essential to ensure that we possess the requisite tools to analyze the evolution of the binary system of interest.

In the second chapter there will be a discussion about the numerical calculations and tools. More precisely we shall present the equations that we used for the python code concerning the accretion process and essentially the spin evolution of the binary. In this thesis we will follow Bhattacharyya implementations for the accretion process [Bhattacharyya, 2021] and the main work is going to be around three different cases of binaries, with a neutron star as the primary star and a main sequence star that will eventually evolve into a millisecond pulsar-white dwarf system, that may differ in initial mass and orbital period. Then we can check if the phase transition is a possibility and what are the consequences of this process.

Chapter 2

Numerical Calculations and Methods

In this chapter we are going to discuss the actual work of this thesis by first referring to the methods we utilize and the calculations we conducted using the proper tools and in the aftermath we shall present the parameters we used for this project. For the purpose of studying the LMXB, there are three important things that can help us understand the characteristics of the LMXB which are:

i) **Stellar evolution**: To achieve a mass transfer detailed profile, we must first know the evolution of our LMXB system (see Section 1.2.4).

ii) **Equation of State**: We need a proper EoS for the neutron star matter that allows the phase transition to happen.

iii) **Accretion process**: In order to calculate the evolution of spin and mass respectively, we, foremost, should study the accretion mechanism, so we shall discuss the theoretical models for the accretion process in subsection 2.4.

2.1 Modules for Experiments in Stellar Astrophysics

Modules for Experiments in Stellar Astrophysics (MESA) is a software program that deals with the theoretical and computational aspects of astrophysics. It was created by Bill Paxton, in collaboration with several astrophysicists, over a period of ten years. MESA is a useful resource for researchers and educators in the astrophysics field, and it is available to the public as open-source software. MESA can solve numerically the differential equations of stellar evolution in 1D and assuming spherical symmetry [Paxton et al., 2010]

$$\left(\frac{\partial m}{\partial r}\right)_t = \frac{1}{4\pi r^2 \rho} \tag{2.1.1}$$

$$\left(\frac{a}{4\pi r^2}\right) = \frac{Gm}{4\pi r^4} + \frac{\partial P}{\partial m} \tag{2.1.2}$$

$$\left(\frac{\partial T}{\partial m}\right)_t = -\frac{Gm}{4\pi r^2}\frac{T}{P}\vec{\nabla}\cdot\left(1 + \frac{r^2}{GM}\frac{\partial v}{\partial t}\right)_m \tag{2.1.3}$$

$$\left(\frac{\partial L}{\partial m}\right)_t = \epsilon_{nuc} - \epsilon_{gr} - \epsilon_\nu \tag{2.1.4}$$

The quantities in the above equations can be described as follows: m is the mass interior to cell, r is the radius at the cell face, ρ is the density, α is the Lagrangian acceleration, G is the gravitational constant, P is the pressure, T is the temperature, M is the total mass, v is the velocity at the cell face, t is the time, L is the total luminosity, ϵ_{nuc} is the nuclear energy generation, ϵ_{gr} is the gravitational energy rate and ϵ_ν is the energy loss from neutrino emission.

Stellar evolution calculations play a crucial role in astrophysics research by providing detailed information about the properties of stars. This information is needed in a wide range of fields, including asteroseismology, nuclear astrophysics, and stellar populations. Despite being a well-established field, there is still much to be discovered about stars, particularly in relation to their three-dimensional features such as convection, rotation, and magnetism [Paxton et al., 2013].

Recent advances in observational technology have increased the demand for precise calculations that take into account factors such as mass, metallicity, and age. Even though research into the three-dimensional

aspects of stars is ongoing, MESA remains an essential resource by providing accurate one-dimensional calculations. These calculations continue to be scientifically and educationally important, and MESA's focus is on delivering precise calculations to benefit researchers and educators in the field of astrophysics [Paxton et al., 2015].

2.2 The ACB5 EoS

As mentioned, in Section 1.1.7, the neutron stars can be interpreted through the equation of state that describes the thermodynamics inside its core. As a result not all neutron stars can be associated with the phase transition process. The EoS referred to as "ACB5" is well-suited for investigating phase transitions in accreting millisecond pulsars. ACB5 is a model that combines four polytropes to describe both nuclear and quark matter within hybrid stars [Alvarez-Castillo et al., 2019].

The polytropic equation of state is a simplified mathematical relationship used to describe the pressure-density relationship in certain types of astrophysical objects, such as stars or compact objects, under specific conditions. It assumes that the pressure and density of the object are related by a power-law equation [O'Boyle et al., 2020]:

$$P(n) = \kappa_i (n/n_0)^{\Gamma_i} \ , \tag{2.2.1}$$

where κ_i is a constant in units of pressure, n_i is the supersaturation density, n_0 is the saturation density which equals the nuclear density of 0.16 fm^{-3} and Γ_i is the polytropic index in one of the density regions labeled from i = 1 up to i=4. We should also mention that the polytropic equation of state is an approximation and may not accurately represent the complex behavior of matter in extreme conditions, such as those found in neutron stars or black holes. It is particularly useful for gaining qualitative insights into the behavior of objects without the need for detailed knowledge of their internal composition and interactions.

The four polytropes in ACB5 have distinct physical interpretations. The first polytrope (i = 1) represents the equation of state of nuclear matter at extremely high densities, specifically, those exceeding normal saturation levels. The second polytrope (i = 2) characterizes a situation where a phase transition occurs at a constant pressure denoted as P_{tr}, with this transition happening within a density range spanning from n_2 to n_3. Polytopes in regions 3 and 4, situated beyond this phase transition, describe dense matter scenarios, such as quark matter. The values for every polytrope for EoS ACB5 are presented in Table 2.1 [Paschalidis et al., 2018].

ACB5 Table			
i	Γ_i	κ_i $[MeV/fm^3]$	n_i $[fm^{-3}]$
1	4.777	2.1986	0.1650
2	0.000	33.969	0.2838
3	4.000	0.4373	0.4750
4	2.800	2.7919	0.7500

Table 2.1: The values for every polytrope for EoS ACB5 are presented here

2.2.1 Mass-Radius Relation

In order to gain the relationship between mass and radius of a static hybrid star we use ACB5 EoS as stated in subsection 2.2. The baryonic mass is conserved during the phase transitions which represents the gravitational mass plus the binding energy [Gao et al., 2020].

By using the interpolation method we calculated the radius ($R_{\rm ns}$) and spin ($f_{\rm ns}$) of the neutron star based on its angular momentum $J_{\rm ns}$ and its mass ($M_{\rm ns}$). The range of values we used is from $J_{\rm ns} = 0.0\ J_0$ to $J_{\rm ns} = 0.45\ J_0$ with step 0.05, where $J_0 = GM^2/c$. When we plot the data that are based on the set of mass-radius-angular momentum, associated with ACB5 EoS, we get the graph depicted in Figure 2.1.

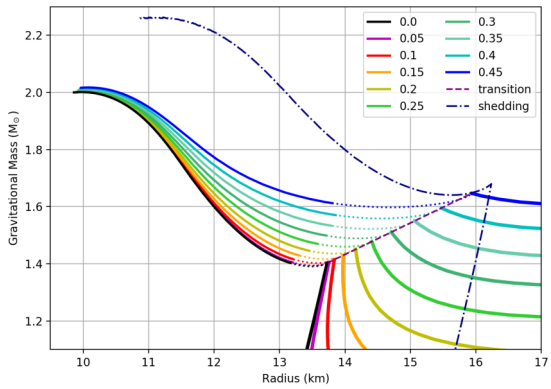

Figure 2.1: Gravitational Mass vs Equatorial Radius. A neutron star initially exhibits a constant angular momentum and increasing mass as it follows a continuous path represented by a solid curve. However, when it reaches a specific transition point (indicated by a dashed line), it becomes unstable and undergoes a rapid phase transition, skipping the trajectory indicated by the dotted curve and transitioning to a different branch known as the "third-family branch". The data for this graph were provided by Victor Danchev. Figure taken from [Ohse, 2021]

2.3 Evolution and Equilibrium of the Orbital Angular Momentum

The orbital angular momentum of a binary system is a conserved quantity, meaning that it remains constant as long as no external torques act on the system. It plays a crucial role in determining the characteristics of the binary system's orbit and can be used to study its dynamics and evolution and help us with our analysis. In 2006 Tauris and Van Den Heuvel presented the following equation for the orbital angular momentum [Tauris and Van Den Heuvel, 2006]:

$$J_{orb} = M_{ns} M_{don} \Omega a^2 \sqrt{1-e^2} \ , \tag{2.3.1}$$

where M_{ns} and M_{don} are the masses of the neutrons star and the donor respectively, Ω is the angular velocity of the system, a is the separation between the neutron star and the companion and e is the eccentricity. For the pre-transition phase, we assume circular orbit, as mentioned before, thus $e = 0$. With a logarithmic differentiation in 2.3.1, results the relation below:

$$\frac{\dot{a}}{a} = 2\frac{\dot{J}_{orb}}{J_{orb}} - 2\frac{\dot{M}_{ns}}{M_{ns}} - 2\frac{\dot{M}_{don}}{M_{don}} + \frac{\dot{M}_{ns} + \dot{M}_{don}}{M} \tag{2.3.2}$$

where the total change in orbital angular momentum is given by: [Misra et al., 2020]

$$\frac{\dot{J}_{orb}}{J_{orb}} = \frac{\dot{J}_{gwr}}{J_{orb}} + \frac{\dot{J}_{mb}}{J_{orb}} + \frac{\dot{J}_{ls}}{J_{orb}} + \frac{\dot{J}_{ml}}{J_{orb}} \tag{2.3.3}$$

The $\dot{J}_{gwr}/J_{orb}$ is the orbital angular momentum due to gravitational wave radiation, the $\dot{J}_{mb}/J_{orb}$ is the orbital angular momentum caused by the magnetic braking, $\dot{J}_{ls}/J_{orb}$ refers to the potential transfer of angular momentum between the orbit and the donor star as a result of changes in the star's size, either when it expands or contracts, while $\dot{J}_{ml}/J_{orb}$ This describes how the loss of mass from the binary system leads to alterations in its orbital angular momentum. Lets analyse a little further.

When a binary system emits gravitational waves, it loses energy and angular momentum. As the objects in the binary system spiral closer together, they accelerate and emit these waves in accordance with Einstein's theory of general relativity. This emission of gravitational waves carries away energy and angular momentum from the system, causing the binary's orbit to decay and the objects to move closer. The angular momentum of the binary system is intimately linked to its orbital properties. As gravitational waves carry away angular momentum, the binary's orbital angular momentum decreases, causing the orbit to shrink. This process continues until the objects eventually merge [Bialynicki-Birula and Bialynicka-Birula, 2016].

$$\frac{\dot{J}_{gwr}}{J_{orb}} = -\frac{32}{5}\frac{G^3}{c^5}\frac{M_{ns} M_{don} M}{a^4} s^{-1} \tag{2.3.4}$$

Magnetic braking in binary systems involves the interaction of magnetic fields between two closely orbiting celestial objects, like stars or compact objects. This interaction results in the exchange of angular momentum, affecting both the orbital dynamics and the rotational evolution of the objects. It can cause the binary orbit to shrink as angular momentum transfers from orbital motion to the objects' spin. Magnetic braking is particularly relevant in systems with strong magnetic fields, like neutron stars and white dwarfs, and it can lead to phenomena such as tidal locking, where an object's rotation synchronizes with its orbital period [Ivanova and Taam, 2003].

The third term, as previously discussed, relates to the spin-orbit coupling effect. Tidal synchronization aims to align the rotational speed of the donor star with the orbital speed of the binary system ($\Omega_{don} = \Omega_{orb}$). When the donor star undergoes expansion or contraction, its moment of inertia (I_{don}) changes accordingly. The spin angular momentum (J_{don}) is represented as $J_{don} = I_{don}\Omega_{don}$. In order to achieve the coordination of the angular velocities, there is an exchange of angular momentum between the donor star and the orbital motion, expressed as $\dot{J}_{ls} = -\dot{J}_{don}$. As a result, we express this term accordingly [Misra et al., 2020]:

$$\frac{\dot{J}_{ls}}{J_{orb}} = -\frac{\dot{I}_{don}\Omega_{don} + I_{don}\dot{\Omega}_{don}}{J_{orb}} \ . \tag{2.3.5}$$

The final component in equation 2.3.1 accounts for the loss of orbital angular momentum due to mass loss, which typically represents the most significant factor influencing the change in angular momentum. Assuming that mass is ejected primarily from the region surrounding the accretor and accounts for a fraction β of the total mass loss, this term can be expressed as:

$$\frac{\dot{J}_{ml}}{J_{orb}} \simeq -\frac{\beta\mu_M^2}{1+\mu_M}\frac{\dot{M}_{don}}{M_{don}} \ , \tag{2.3.6}$$

where $\mu_M = M_{don}/M_{ns}$.

2.4 Spin Evolution

To better grasp the model's characteristics, one should utilize certain measurements for calculations. Specifically, three different lengths will be needed for this analysis [Bhattacharyya, 2021].

i) **Light Cylinder Radius:** The light cylinder is a hypothetical limit around a spinning neutron star where the plasma cannot rotate with the star without surpassing the speed of light. Inside this boundary, the magnetic field is predominantly dipolar, while beyond it, the field lines adopt an increasingly azimuthal configuration as they extend away from the neutron star. The radius of the light cylinder, determined by the equation [Miller, 2010]:

$$R_{\rm lc} = c/\Omega, \ \Omega = 2\pi f_{\rm ns} \tag{2.4.1}$$

(where c is the speed of light, Ω is the angular velocity of the star's rotation, and $f_{\rm ns}$ is the neutron star's frequency), defines this boundary. If we replace Ω, by definition we get the following equation:

$$R_{\rm lc} = \frac{c}{2\pi f_{\rm ns}}. \tag{2.4.2}$$

ii) **Magnetospheric Radius:** Neutron stars have extremely strong magnetic fields, much stronger than those of ordinary stars. The magnetospheric radius ($R_{\rm mag}$) refers to the distance from the center of the neutron star at which the pressure from the magnetic field balances the ram pressure from the infalling material (typically from an accretion disk) trying to approach the neutron star. It's the point where the magnetic field becomes dynamically significant in governing the behavior of matter around the neutron star. The equation that represents this radius according to [Tauris, 2012] is the following:

$$R_{\rm mag} = B^{4/7}R_{\rm ns}^{12/7}\dot{M}^{-2/7}(2GM_{\rm ns})^{-1/7} \ , \tag{2.4.3}$$

where B is the magnetic field, $R_{\rm ns}$ is the radius of the neutron star, $\dot{M}$ is the mass

iii) **Corotation Radius:** Is defined as the distance where the angular velocity (Ω), of the neutron star and its accreating disk, is equal to the Keplerian angular velocity [Romanova and Owocki, 2015]. So the corotation radius is given by the following equation:

$$R_{\rm co} = \frac{(GM_{\rm ns})^{1/3}}{(2\pi f_{\rm ns})^{2/3}} \ . \tag{2.4.4}$$

A quantity that assists in the examination of the accretion process needs to be defined. This quantity is called fastness parameter and is defined as the ratio of the angular velocity of the neutron star to the Keplerian angular velocity of the accreting disk at the magnetic radius. [Tauris et al., 2012]

$$\omega = \frac{\Omega_{\rm ns}}{\Omega_{\rm K}(R_{\rm mag})} \Rightarrow \omega = \frac{2\pi f_{\rm ns}}{\sqrt{\frac{GM}{R_{\rm mag}^3}}} \Rightarrow \omega = \left(\frac{R_{\rm mag}}{R_{\rm co}}\right)^{3/2} . \tag{2.4.5}$$

In the context of accretion disks around compact objects, the fastness parameter is essential in understanding the accretion process. If the parameter is less than one, it means the star's rotation is slower than its orbital motion, and the accretion process can occur efficiently (**accretion phase**). However, if the parameter exceeds one, the star's rotation becomes faster than its orbital motion, which can hinder the accretion process (**propeller phase**). Now if ω is equal to 1, we have reached the **spin equilibrium** phase with the equilibrium frequency to be equal [Tauris et al., 2012]:

$$f_{\rm eq} = \frac{1}{2\pi}\frac{GM}{R_{\rm mag}^3} . \tag{2.4.6}$$

We can now rewrite the fastness parameter as the ratio of the frequency of the neutron star to the equilibrium frequency, $\omega = f_{\rm ns}/f_{\rm eq}$.

Accretion Torque Computation: Tauris' Theoretical Framework

Tauris in 2012 discussed how a neutron star's magnetic field interacts with accreted material, generating torque that can either accelerate or decelerate the star's rotation [Tauris, 2012]. It highlights the potential for torque reversal under specific conditions when mass-transfer rates decrease. Additionally, it notes that low-mass X-ray binaries undergo a phase of stable mass transfer, significantly speeding up the neutron star's rotation to milliseconds. He also describes their method of integrating both approaches to calculate torque and track its impact on the pulsar's spin rate during the mass-transfer phase's conclusion. The equation that calculates the accretion torque [Tauris, 2012]:

$$N(t) = n(\omega)\left[\dot{M}(t)\sqrt{GM_{\rm ns}R_{\rm mag}(t)} + \frac{\mu^2}{9R_{\rm mag}^3(t)}\right] - \frac{\dot{E}_{\rm dip}(t)}{\Omega_{\rm ns}(t)} . \tag{2.4.7}$$

The quantities in the above equation can be described as follows: $n(\omega)$ is a dimensionless function depending on ω and is represented by equation 2.4.8 while ω is the fastness parameter, $\dot{\rm M}$ is the mass transfer rate, G is the gravitational constant, $M_{\rm ns}$ is the mass of the neutron star, $R_{\rm mag}$ is the magnetic radius, μ is the dipole moment, $\dot{E}_{\rm dip}$ is the magnetic lose and $\Omega_{\rm ns}$ is the angular velocity of the neutron star.

$$n(\omega) = tanh\left(\frac{1-\omega}{\delta\omega}\right) \quad \text{and} \quad \mu = BR_{ns}^3 \quad . \tag{2.4.8}$$

Accretion Torque Computation: Bhattacharyya's Theoretical Framework

Bhattacharyya later in 2021 suggested that a slight decrease in the spin frequency (ν) of millisecond pulsars might explain why MSPs within Low-Mass X-ray Binaries have higher ν-values compared to those in the post-LMXB phase [Bhattacharyya, 2021]. He proposed that this decrease in frequency could be due to temporary accretion during the Roche Lobe Decoupling Phase (RLDP), a stage where, as mentioned in subsection 1.2.2, mass transfer becomes less efficient in binary systems. Despite this decrease, ν should not become extremely low, even if the mass transfer rate ($\dot{M}$) slows down to zero as the LMXB phase ends. The evolution of ν is complex, offering various possibilities and pathways for change over time [Bhattacharyya, 2021]. So the accretion torque is now given by the following equation:

$$N_{\mathrm{T12}} = \begin{cases} \dot{M}\sqrt{GM_{\mathrm{ns}}R_{\mathrm{mag}}} + \dfrac{\mu^2}{9R_{\mathrm{mag}}^3}(3 - 6\omega + 2\omega^2) - \dfrac{\dot{E}_{\mathrm{dip}}}{\Omega_{\mathrm{ns}}} & for\ \omega < 1 \\ -\dfrac{\dot{E}_{\mathrm{dip}}}{\Omega_{\mathrm{ns}}} & for\ \omega = 1 \\ \dot{M}\sqrt{GM_{\mathrm{ns}}R_{\mathrm{mag}}} - \dfrac{\mu^2}{9R_{\mathrm{mag}}^3}(3 - 2\omega^{-1}) - \dfrac{\dot{E}_{\mathrm{dip}}}{\Omega_{\mathrm{ns}}} & for\ \omega > 1 \end{cases} \tag{2.4.9}$$

2.5 The parameters for this project

In order to begin our calculations and analysis we first need to use MESA to simulate the evolution of a binary system consist of a neutron star as a point mass and main-sequence star as its companion. The data sets we used for this projects differ in mass and period but have the same metallicity and the percentage of helium burning $Z = 0.02$, $b = 0.5$ respectively. Also the magnetic field that we used at the evolution code, is set at $B = 10^8$ *Gauss* which is a typical value for neutron stars. So we used the collected data and used all the equations mentioned before to write the evolution to analyze them.* To extract the necessary data for the pulsar, we use the ACB5 Eos as a base for the neutron stars core. In this context we interpolated the radius and the frequency of the neutron star using the relation that these data had between mass, radius, angular momentum and frequency.

Essentially, there we be a display of three different cases. In the first case the system is not able to achieve the phase transition, in the second case the phase transition occurs during the mass transfer, while in the third we see a phase transition after the mass transfer ends. So for each case (i is the index that suggest the number of case) we choose initial values for the donor's mass (M_{d}), the neutron star's mass (M_{n}), and the orbital period (P_{orb}) The values are displayed in the following table (Table 2.2).

Parameters Table			
i	M_{d} $[M_\odot]$	M_{n} $[M_\odot]$	P_{orb} [days]
1	1.0	1.0	8
2	1.0	1.2	8
3	1.0	1.2	22.627

Table 2.2: The values of the different parameters are presented here

*The simulation and the data collection where made by David Ohse.

Chapter 3

Results

In this chapter, the results of the project will be discussed, accompanied by an analysis of the characteristics of the different cases that were investigated.

3.1 First Case: No Phase Transition

The simulation runs and calculates the data for the neutron star and the MS companion start. As long as the companion star is in the MS phase, the binary system will evolve "smoothly". When the donor star enters the red-giant branch, will start fill the Roche-lobe after approximately 12.2 Gyrs. From this point on the neutron star accretes matter from the donor star with a mass transfer rate of $\dot{M} \simeq 10^{-7}\ M_{\odot}\ \mathrm{yr}^{-1}$ (see Figure 3.3a). The pulsar will immediately spun up, due to the accretion mechanism, with a spin period $P_{ns} \simeq 1.1$ ms and from this moment on, the orbital period which is initially $P = 8$ days will start increase by time (see Figure 3.3d).

For this case, we plotted the Roche-lobe radius (km) and donor radius (km) over time (Gyrs), in order to define the important areas of the evolution that have been mentioned in Section 1.2.2(Figure 3.1).

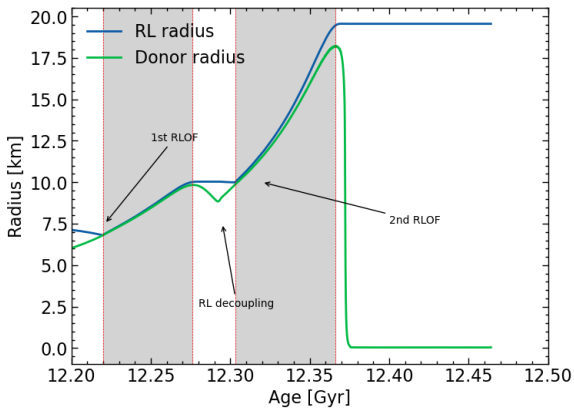

Figure 3.1: Radius VS Age first case.

At the first point where the donor mass equals the Roche-lobe radius, is the beginning of the first Roche-lobe overflow. From this point on until the two radius star "separating", when the reach the first maximum, we see the 1st RLOF area, which will last for approximately 58 Myrs. When the first separation occurs the Roche-lobe decoupling phase takes place until the two radius take the same value once again. For that period of time $\sim$ 28 Myrs the pulsar will enter a propeller phase in which the spin period will be stable with a mean value of $< P_{spin} >= 3.45$ ms. Also the mass transfer and the torque stop, the mass of the pulsar $M_{\mathrm{ns}} = 1.22\ M_{\odot}$ while the orbital period is $P_{orb} \sim 16.5$ days. Then the second RLOF begins up until the RL and the donor radius take the maximum value of 19.6 and 18 km respectively. The mass transfer and torque initiate once again and while this time the spin period only achieves a minimum value of 2.1 ms. The orbital period increases dramatically in comparison to the 1st RLOF. The 2nd RLOF will last for approximately 63 Myrs. Last but not least the final propeller phase begins at the end of the 2nd RLOF and exist until the end of the evolution where the orbital period is stabilizes at 60 days, the final mass and radius of the neutron star are 1.31 $M_{\odot}$ and 13.9 km respectively while the spin period relaxes at 3.3 ms. So as we have established the significant areas of evolution and we can proceed further with our analysis.

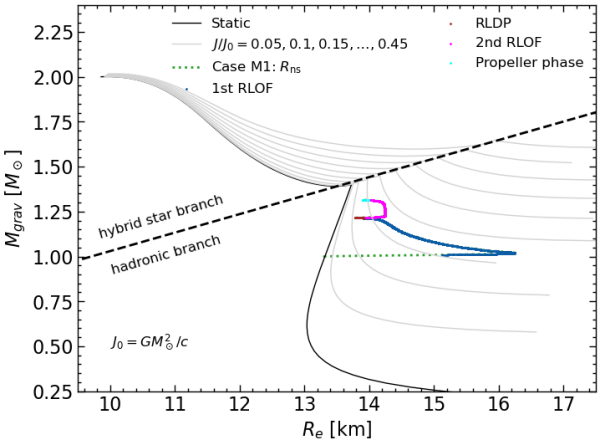

(a) Phase transition for the first case.

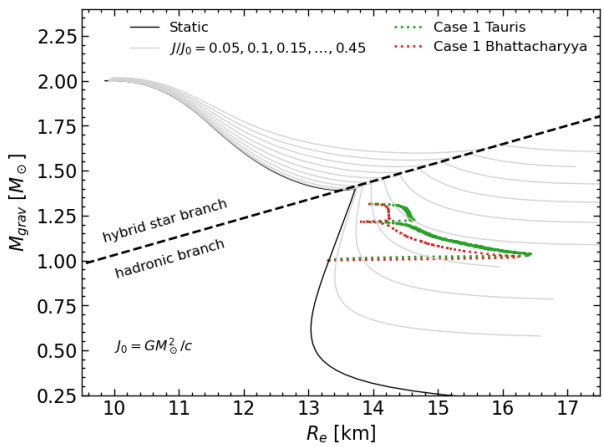

(b) Comparison between Tauris' and Battacharyya's computation for the first case.

For the case of $M_{\rm n} = 1\ M_\odot$, $M_{\rm d} = 1\ M_\odot$, and $P_{\rm orb} = 8$ days, we plot the radius-mass graph to check if the pulsar can surpass the hadronic branch limit through the phase transition process and become a hybrid star (see Subsection 2.2.1). We specified the different stages of evolution the 1st RLOF, RLDP, 2nd RLOF, and final propeller phase. We can see that the system does not have the necessary qualifications in order for a phase transition to occur as it can not surpass the limit of pure hadronic mass in both computations. The system begins with a mass of $M_{\rm ns} = 1\ M_\odot$ and radius of $R_{\rm ns} = 13.2$ km, while it ends its evolution with a mass of $M_{\rm ns} = 1.31\ M_\odot$ and radius of $R_{\rm ns} = 13.9$ km. The donor that is now a white dwarf, has a mass of $0.29\ M_\odot$.

After we established that for this case the phase transition is not happening in the evolution of the binary, we plotted the following four graphs.

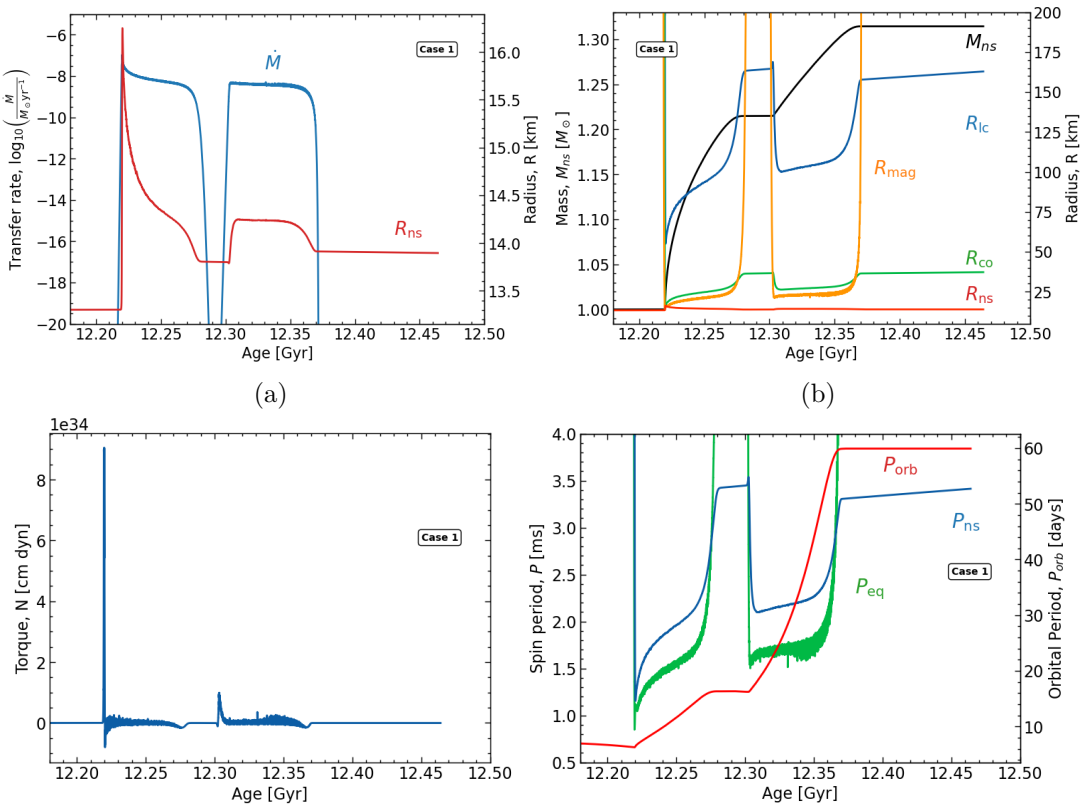

Figure 3.3: Plots for the no phase transition case. Panel 3.3a depicts the mass transfer rate/radius over time, Panel 3.3b portrays the mass/radius-age plot, Panel 3.3c presents the torque-age graph, and Panel 3.3d illustrates the spin/orbital period over time graph.

We can see the change in mass, mass transfer and all the radial quantities we used due to Roche-lobe

overflow (3.3a, 3.3b. Is very clear that the radius of the neutron star fluctuates only for a couple of kilometers (from 13.3 to a maximum of 16 until it eventually stabilized in 13.9 km) in comparison to the other quantities that represent a radii units ($R_{\rm cor}$, $R_{\rm lc}$, $R_{\rm mag}$) where the fluctuation is much more significant and has a greater range.

On the other two figures we see the fluctuation in torque and spin period (3.3c, 3.3d respectively) again match the Roche-lobe overflow. Torque will fluctuate in a small range, until it resets to zero. In the spin/orbotal period-age graph we present not only the neutron star spin period but also the equilibrium spin period. The stabilization of the fluctuation for the P_{ns} occurs at around 3.4 ms.

So in overall we have calculate and plotted some important values and quantities for a case that the phase transition does not meet the right conditions.

3.2 Second Case: Phase Transition During the Evolution

In the second scenario we slightly increase the neutron star's mass from 1 $M_\odot$ to 1.25 $M_\odot$ and we want to see what will differ from the previous case. For the second case we will follow the same process of analysis and we shall compare with the first case. By following the same steps as we did in the first case, we created the following graph.

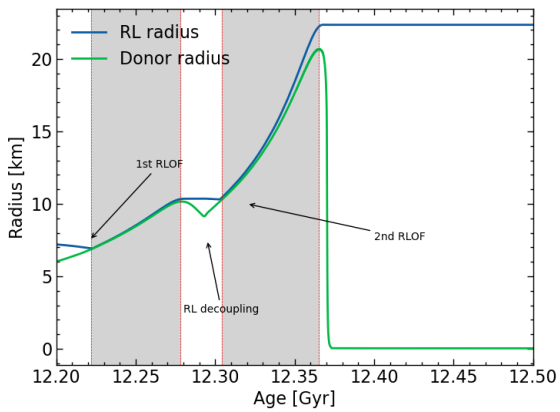

Figure 3.4: Radius VS Age second case.

We detect identical areas of evolution with similar values as the first case and an identical time duration for each area. In this scenario the RL radius stabilizes at the end of the evolution at higher values (22.36 km) and the donor radius reaches a higher peak than previously (19.56 km). Due to the increase of inital mass for the neutron star, their has been a change in the 4 graphs depicted in Figures 3.6a-3.6d. More accurately, the mass transfer initiates with a value of $\dot{M} = 10^{-7.5}\ M_\odot\ yr^{-1}$ and the radius of the pulsar at 13.6 km. Additionally, the spin up of the pulsar will grant it with a spin period of 1.5 ms. After the RLDP the mass, radius spin period of the neutron star, and orbital period will be almost stable with respective values of 1.39 $M_\odot$, 14.1 km, 2.9 ms and 16 days. Then again due to the RLOF the values will start fluctuate until the final propeller phase where the system will "rest".

At this point, for the case of $M_{\rm ns} = 1.25\ M_\odot$, $M_{\rm don} = 1\ M_\odot$ and $P_{\rm orb} = 8\ days$ we plot the radius with mass in the graph that represents different cases of angular momentum J and can provide use with the information of phase transition that we mentioned in subsection 2.2.1.

This graph looks very similar with the one in the first case, but is shifted upwards (vertical axes) as it starts with a different mass. This difference in initial mass, makes the system capable of led to a phase transition process, during the second Roche-lobe overflow. We can see that for this case, the phase transition occurs at mass $M_{\rm ns} = 1.47\ M_\odot$ and radius $R_{ns} = 14.25$ km during the evolution of the binary.

Once again we plotted the following four graphs as we did in the first case.

The four graphs have also a similar form as the ones in the first case. More precisely, in the first Roche-lobe overflow the graphs are almost identical. However when we reach the second Roche-lobe due to the phase transition occurring the graphs take a different turn than before. We can see that fluctuation in all four graphs is more significant than before. The radius of the neutron star takes higher values in the 2nd RLOF and all the other important lengths have a slight decrease. The torque and the spin has a higher fluctuation although the former take higher values and the latter lower than before. The spin period of the neutron star, $P_{\rm ns}$ starts having a smoother increase at 2.25 ms, a smaller value than the first case.

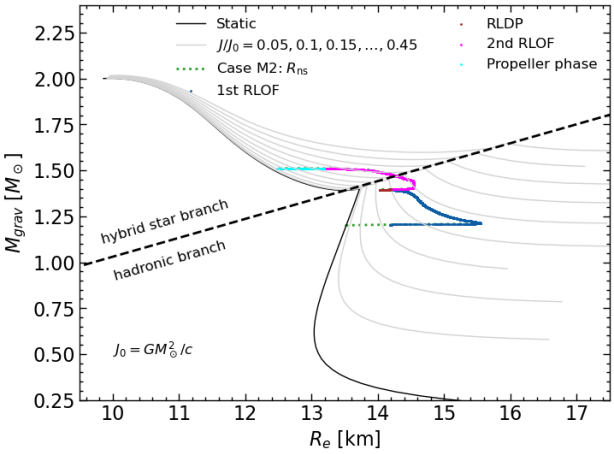

(a) Phase transition for the second case.

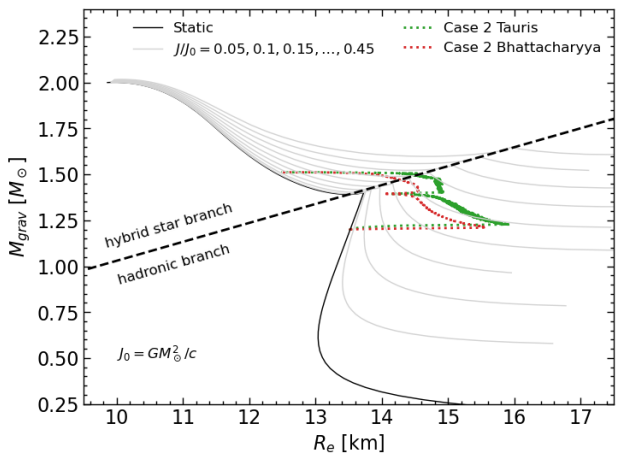

(b) Comparison between Tauris' and Battacharyya's computation for the second case.

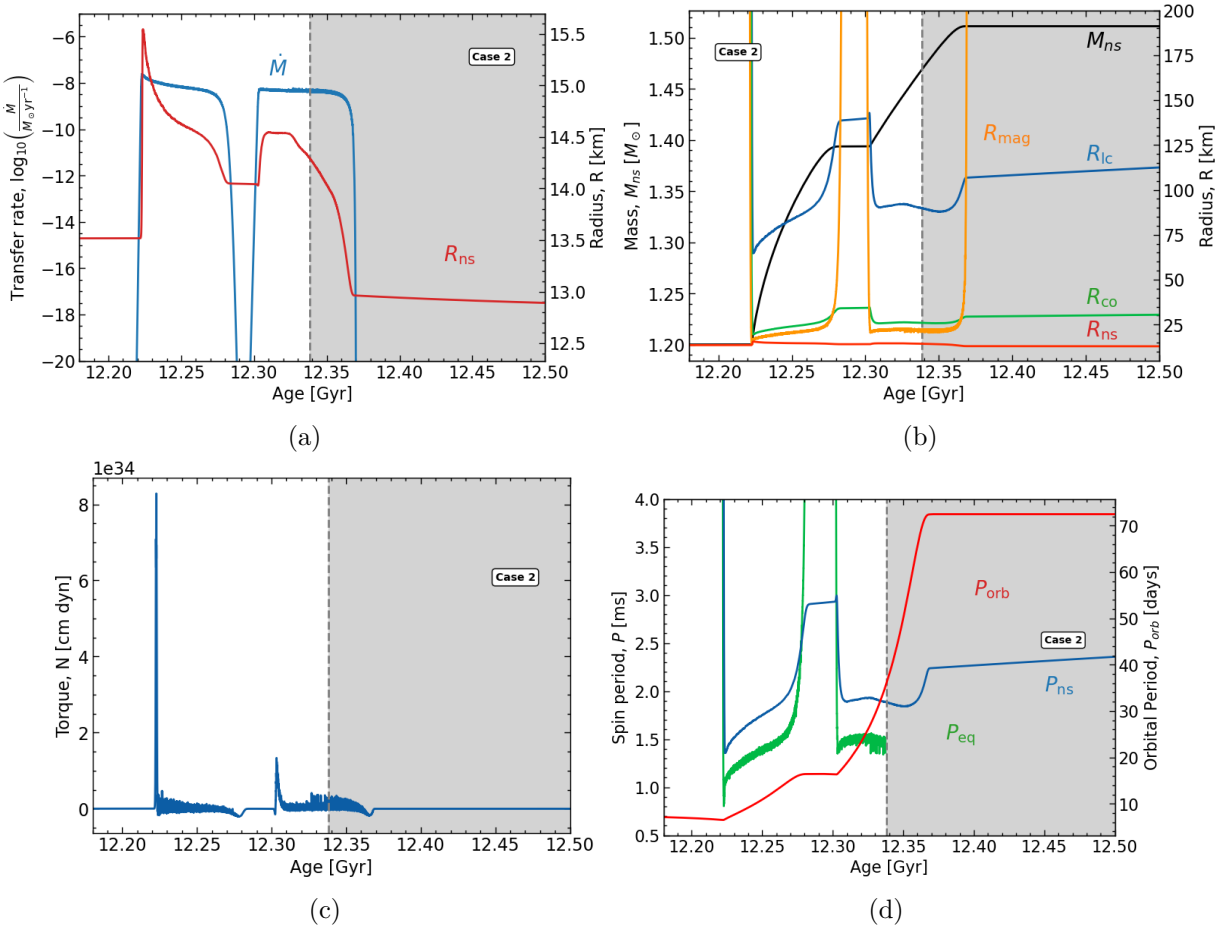

Figure 3.6: Plots for the case of phase transition during the mass transfer. Panel 3.6a depicts mass transfer rate/radius over time (age), Panel 3.6b presents a mass/radius-age plot, Panel 3.6c portrays a torque-age graph, and Panel 3.6d illustrates a spin/orbital period over age graph. The dashed line represents the point where the phase transition occurs, and the area from this point on is colored with grey.

The final values for the mass and radius of the neutron star are $M_{\rm ns} = 1.51\ M_\odot$, $R_{\rm ns} = 13.9$ km and for the donor that is now a white dwarf, $M_{\rm don} = 0.30\ M_\odot$. The spin period and orbital period will "relax" accordingly, with approximately values of $P_{\rm ns} \sim 2.4$ ms and $P_{\rm orb} \sim 73$ days.

So we can conclude that the increase in the mass of the neutron star is a key factor to weather the phase transition can happen to the binary system we study. To be more accurate, if we increase the primary star's initial mass, we increase the chance of the phase transition and consequently have the possibility of transform the neutron star into a hybrid star.

3.3 Third Case: Phase Transition After the Evolution Ends

Last but not least we shall analyse a third case of the type of binary that is mentioned through this thesis. Once again we will need the graph of Radius vs Age to detect the important areas we need.

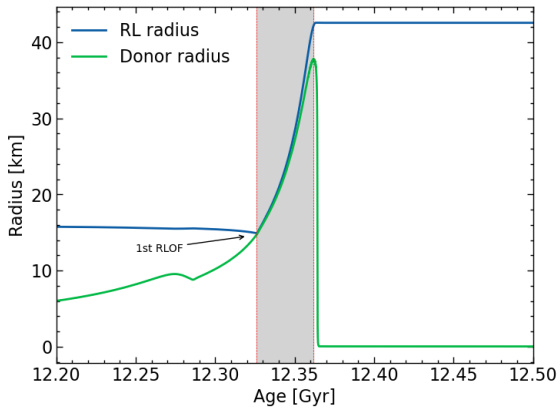

Figure 3.7: Radius VS Age third case.

We can detect only one Roche-lobe overflow in this case in deference with the previous two cases. In this scenario the main sequence star will fill its Roche-lobe after approximately 12.32 Gyrs which will initiate a mass transfer from the MS star to the neutron star with initial value of $\dot{M} = 10^{-7.5}\ M_{\odot}\ yr^{-1}$. The pulsar of 1.25 solar masses, at this point has the following values for radius and spin period: $R_{\rm ns} = 13.5$ km and $P_{\rm ns} \sim 1.2$ ms. The RLOF will endure for about 30 Myrs and then the propeller phase will follow. The aforementioned quantities will reach final values of $M_{\rm ns} = 1.49\ M_{\odot}$, $R_{\rm ns} \sim 13.4$ km, $P_{\rm ns} \sim 2.1$ ms, and $P_{\rm orb} = 180$ days. Also the Roche-Lobe radius in this case reaches stabilization at $RL_{\rm max} = 42.55$ km and the white dwarf will have a mass of $M_{\rm don} = 0.33\ M_{\odot}$.

In the scenario where $M_{\rm ns} = 1.25\ M_{\odot}$, $M_{\rm don} = 1\ M_{\odot}$ and $P_{\rm orb} = 22.627$ days we generate a graph depicting the relationship between radius and mass, considering, once again, various angular momentum (J) cases. This graph serves as a visual representation of the different instances discussed in subsection 2.2.1, offering insights into the phase transitions associated with these conditions.

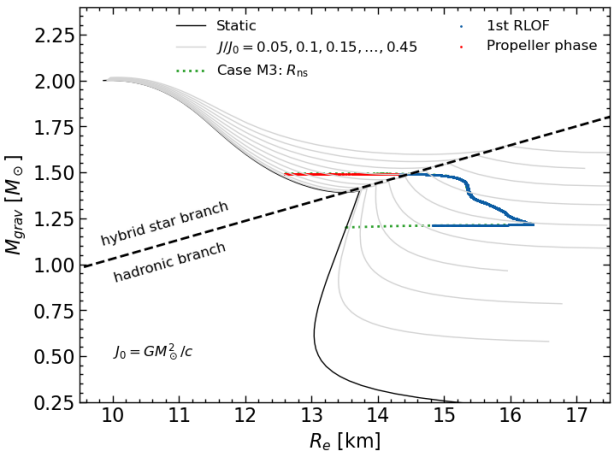

(a) Phase transition for the third case.

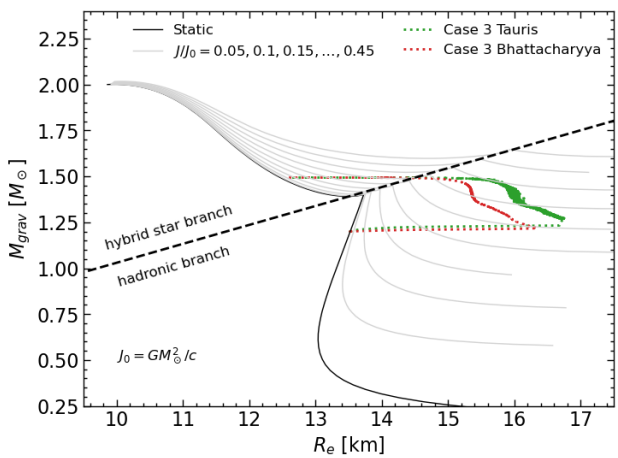

(b) Comparison between Tauris' and Battacharyya's computation for the third case.

In comparison with the second case, the phase transition occurs after the end of the mass transfer from the companion to the neutron star. So the increase of the period led to one Roche-lobe overflow and consequently to the phase transition at the beginning of the propeller phase. The phase transition occurs at mass $M_{\rm ns} = 1.49\ M_{\odot}$ and radius $R_{\rm ns} = 14.4$ km.

In summary, boosting the spin period of the neutron star is crucial for determining whether a phase transition can occur in the binary system under investigation. More precisely, raising the initial period of the central star enhances the likelihood of the phase transition, ultimately resulting in the transformation of the neutron star into a hybrid star.

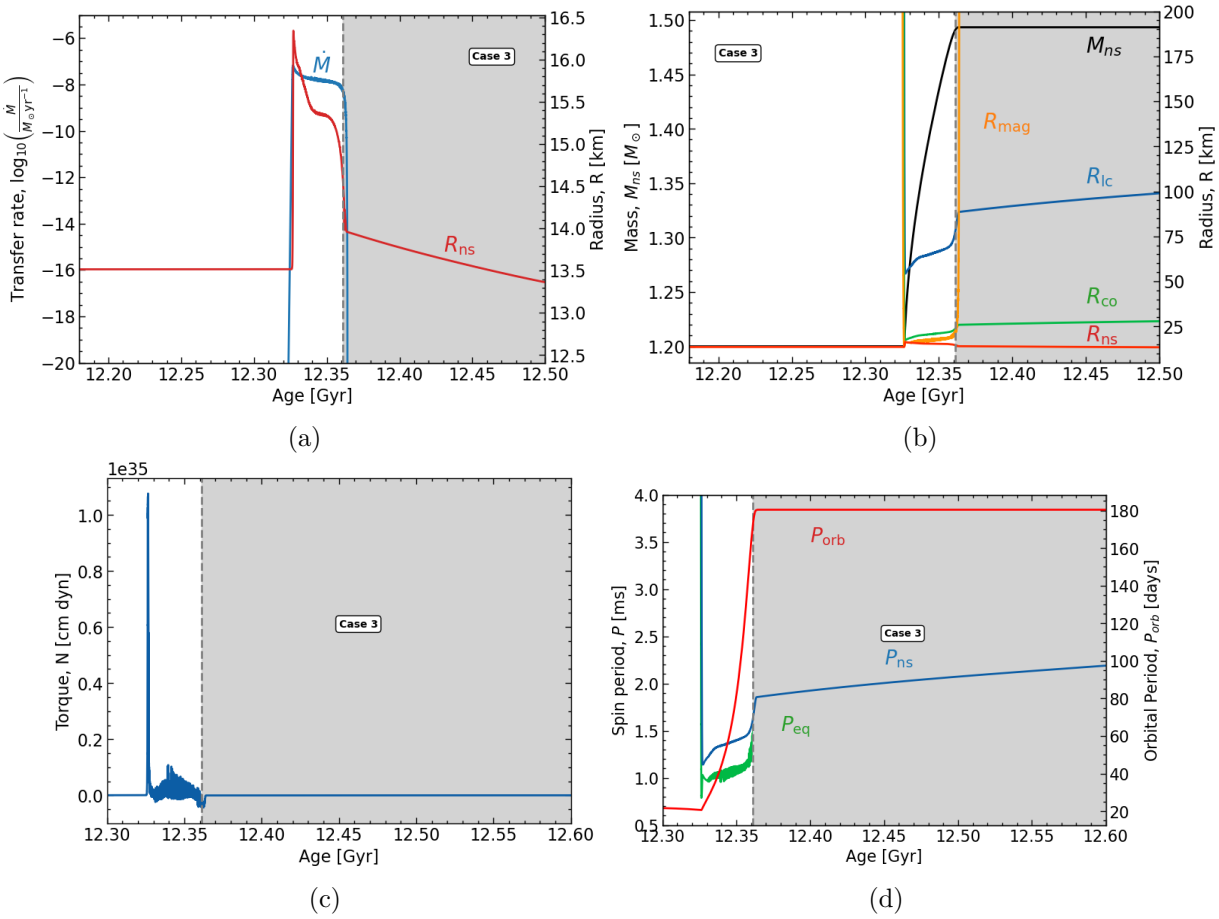

Figure 3.9: Plots for the case of post mass transfer phase transition. Panel 3.9a depicts mass transfer rate/radius over time (age), Panel 3.9b presents a mass/radius-age plot, Panel 3.9c illustrates a torque-age graph, and Panel 3.9d portrays a spin/orbital period over age plot. The dashed line represents the point where the phase transition occurs, and the area from this point on is colored with grey.

3.4 Comparison of All Three Cases

At this section there shall be the comparison of the three cases that were discussed above. The presentation of the final graph, with all cases together, can provide information about the 1st order phase transition (Figure 3.10.

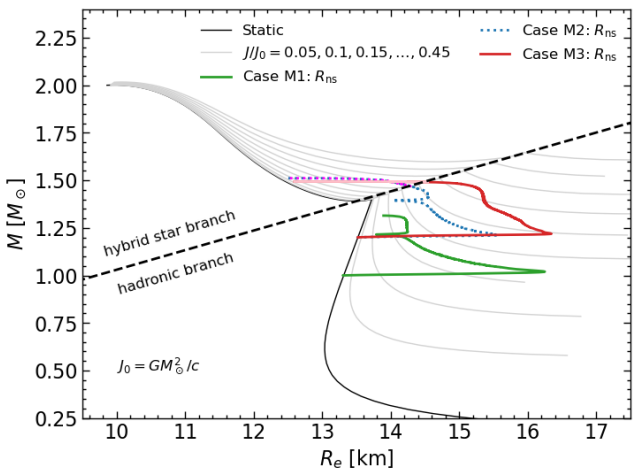

Figure 3.10: Phase transition for all cases. The three cases are marked with different colours (1, 2 and 3 with green, blue and red respectively) and for the cases that lead to the phase transition the colour is changed (2 and 3 to magenta and pink respectively).

The second case, which only differs in the mass of the neutron star from the first case, appears almost

identical but shifted upwards in the vertical axes. On the other hand the third case that differ from the second only in the period, looks like is shifted to the right in the horizontal axes, but does not have the exact same structure (probably due to having only one Roche-lobe overflow).

At this section, it should also be mentioned that the graphs after the phase transition in cases 2 and 3 are not correct. That happens because, as it is already been established in section 1.3, the gravitational mass is not conserved during the phase transition, only the baryonic mass does not change. So in order for the evolution to be correct, the need of a different set of data concerning the baryonic mass is necessary to portray the correct mass.

3.5 Eccentricity and Orbital Reconfiguration

As was stated before, in order to the check if the millisecond pulsar becomes an eccentric one, after the phase transition process, the need for the values of eccentricity and orbital reconfiguration is necessary. Although the analysis in this thesis ends here, similar work has been done (following Tauris' implementations instead of Battacharyya's) in the soon to be published paper by S.Chanlaridis et.al [Chanlaridis et al., prep]. In this analysis, essentially continuing the work that stopped in this thesis, there is also the post-phase transition examination. For this purpose the use of Monte Carlo simulations is needed to simulate what the values of eccentricity and orbital period. Before the simulation was conducted, the hypotheses for mass loss was essential, thus for both cases were the phase transition could occur, the $\Delta M = 0.001\ M_{\odot}$ and $\Delta M = 0.013\ M_{\odot}$. The simulation ran with different values for kick velocity of 0, 5, 10, 15, 20, 50, and 100 km/s, which will compute the post-phase transition the values of eccentricity and orbital period, (see Section 1.3.1). The hypothesis at these point is that the results using Battacharyya's computation is very similar to the one's using Tauris implementations and thus we can assume similar results for the aforementioned quantities. In both scenarios where the phase transition occurred, when there is no kick velocity, the orbit of the binary becomes slightly eccentric solely due to gravitational mass loss. The neutron star's mass loss during the phase transition induces a modification in the gravitational potential, resulting in a departure from circularity in the orbit [Chanlaridis et al., prep]. With low kick velocities the eccentricity experiences a moderate increase but remains relatively modest. However, as the kick velocity escalates, the distribution peak shifts towards higher eccentricities, and the distribution widens, indicating a wider array of potential post-kick orbits. Wider binary systems, exemplified by case 3, tend to produce orbits with greater eccentricity at higher kick velocities compared to compact binaries, like case 2. In extreme cases, wider binaries might even undergo disruption, leading to the formation of isolated millisecond pulsars (see Section 1.2.4). These differences between case 2 and case 3 suggest that the timing of the phase transition, whether during mass accretion or spin down, significantly influences the resulting eccentricity and orbital outcomes [Chanlaridis et al., prep].

These simulations suggest that the kick resulting from a sudden mass loss of approximately 0.001 solar masses is insufficient to explain neutron stars with eccentricities on the order of 0.1. In such instances, supplementary mechanisms like the rocket effect or neutrino-driven kicks, or additional factors, would be necessary to adjust the outcomes and achieve the desired eccentricity. Alternatively, an eccentricity of around 0.1 could be attained without requiring an additional kick mechanism if, during the transition, the mass loss is about 0.01 $M_{\odot}$ [Chanlaridis et al., prep]. However, while it is feasible to generate the desired eccentricity range, achieving both the desired eccentricity and an orbital period of 20 to 50 days simultaneously might be less common, particularly as configurations with the appropriate eccentricity and shorter orbital periods within that range are sparsely distributed. Nonetheless, this scenario remains plausible, especially when considering potential secondary effects and the inherent uncertainties associated with such intricate astrophysical systems [Chanlaridis et al., prep].

Chapter 4

Conclusion

To conclude this thesis, we start this project in order to give an explanation in the eccentric millisecond pulsars formation and their peculiar behavior. The theory we try to prove or disprove, is based on the phase transition in matter in which the protons and neutrons inside the neutron star, due to extreme conditions of pressure and temperature, will decay into quark matter. This intense procedure will grant the system with enough energy to trigger an asymmetric kick that will set the orbit of the binary to an elliptic one.

Now in order to test this theory we used a software program, MESA, to create a simulation about the evolution of a low-mass binary system with a neutron star as the primary star and a star in the main-sequence, that eventually will become a white dwarf, as the companion star. This simulation can provide us with all the important values like mass, radius etc, by solving numerically the differential equations of stellar evolution. After collecting the necessary data, we proceeded by import them in the evolution code we wrote in python that concerns the spin evolution and accretion torque due to mass transfer from the companion to the pulsar.

We studied three different cases of binaries system consist of a neutron star treated as a mass point and a main sequence star as its companion. We first established some standard parameters such us metallicity and the percentage of helium burning at $Z = 0.02$, $b = 0.5$ respectively. Also the magnetic field that was used in code for the spin evolution and accretion torque was set at $B = 10^8$ $Gauss$.

The results of the three cases can show us that the increase of the initial mass of the neutron star and the time period are directly linked with whether the binary will can provide a phase transition process to the MSP or not. More accurately the increase in those two quantities will make the system more capable of essentially make the neutron star a hybrid star. After assumptions about the mass loss and the hypothesis that both computation methods for the accretion torque give similar results, we present the further analysis that was made by [Chanlaridis et al., prep] in which Tauris methodology was tested. After hypothesis for the mass loss and with the use of Monte Carlo simulations, testing different values for the kick velocity (0-100 km), they were lead to the following conclusions. For a mass loss of 0.001 $M_\odot$ the phase transition can not be responsible for the creation of an eccentric millisecond pulsar, with 0.1 eccentricity, without an additional mechanism. For a mass loss of 0.01 $M_\odot$ the assymetric kick can from the phase transition can lead to an EMSP with e=0.1 but in range of 20-50 days for the orbital period the cases are extremely rare.

Of course we have to make a more extended analysis with more cases/data in order to have a better understanding on the phase transition process and more precisely if that is the only reason behind the eccentric MSPs. There should also be a larger variety of parameters such as magnetic field, metallicity etc. In addition we need to use Monte Carlo simulations to derive result for the data set that was achieved using Battacharyya's accretion torque computation method. Last but not least the baryonic mass data set will be extremely useful as it will "fix" the phase transition graphs and contribute to a better analysis.

Acknowledgments

I would like to thank Dr John Antoniadis for taking me in his group and accepted to be my supervisor for this thesis.
I would also like to thank Savvas Chanlaridis for not only helping me understand the project but also for the time he spend on this despite already having a ton of work of his own. Also I want to thank him for providing important notes and tips associate the project (DELETE WINDOWS AND INSTALL LINUX!!!!).
I express my gratitude to David Ohse for his work for his own master's thesis that gave the spark for this thesis to become true.
A big thanks to our group's, SALT, members: David, Michael, George, Anna, Maria.
A huge thanks to Maria Peraki for always been there for me and thinking more clear when it was needed.
I would like to thank my dog for the emotional support. (Coco sends her love).
I would like to thank my tricking group for all the flips that gave me the boost I needed.
My family for not only the economical but also for the emotional support.
My friends for always being there for me, in happiness and sadness and would help address problems in life and get through them.
I would also like to thank my physicists heroes that inspired me to follow this path.

Chapter 5

Bibliography

[Alcock et al., 1986] Alcock, C., Farhi, E., and Olinto, A. (1986). Strange stars. *Astrophysical Journal, Part 1 (ISSN 0004-637X), vol. 310, Nov. 1, 1986, p. 261-272.*, 310:261–272.

[Alvarez-Castillo et al., 2019] Alvarez-Castillo, D. E., Antoniadis, J., Ayriyan, A., Blaschke, D., Danchev, V., Grigorian, H., Largani, N. K., and Weber, F. (2019). Accretion-induced collapse to third family compact stars as trigger for eccentric orbits of millisecond pulsars in binaries. *Astronomische Nachrichten*, 340(9-10):878–884.

[Antoniadis, 2014] Antoniadis, J. (2014). On the formation of eccentric millisecond pulsars with helium white-dwarf companions. *The Astrophysical Journal Letters*, 797(2):L24.

[Antoniadis et al., 2016] Antoniadis, J., Kaplan, D. L., Stovall, K., Freire, P. C., Deneva, J. S., Koester, D., Jenet, F., and Martinez, J. G. (2016). An eccentric binary millisecond pulsar with a helium white dwarf companion in the galactic field. *The Astrophysical Journal*, 830(1):36.

[Berdermann et al., 2006] Berdermann, J., Blaschke, D., Grigorian, H., and Voskresensky, D. (2006). Asymmetric neutrino propagation in newly born magnetized strange stars; grb and kicks. *Progress in Particle and Nuclear Physics*, 57(1):334–342.

[Bhattacharyya, 2021] Bhattacharyya, S. (2021). Spin evolution of neutron stars in two modes: implication for millisecond pulsars. *Monthly Notices of the Royal Astronomical Society: Letters*, 502(1):L45–L49.

[Bialynicki-Birula and Bialynicka-Birula, 2016] Bialynicki-Birula, I. and Bialynicka-Birula, Z. (2016). Gravitational waves carrying orbital angular momentum. *New Journal of Physics*, 18(2):023022.

[Carroll and Ostlie, 2017] Carroll, B. W. and Ostlie, D. A. (2017). *An introduction to modern astrophysics*. Cambridge University Press.

[Cassinelli, 1979] Cassinelli, J. P. (1979). Stellar winds. *Annual Review of Astronomy and Astrophysics*, 17(1):275–308.

[Chanlaridis et al., prep] Chanlaridis, S., Ohse, D., Aspradakis, N., Antoniadis, J., Blaschke, D., Alvarez-Castillo, D. E., Danchev, V., and Langer, N. (prep). Astrophysical consequences of dense matter phase transitions i. formation of hybrid stars in low-mass x-ray binaries. *Astronomy and Astrophysics*.

[Cordes et al., 2004] Cordes, J., Kramer, M., Lazio, T., Stappers, B., Backer, D., and Johnston, S. (2004). Pulsars as tools for fundamental physics & astrophysics. *New Astronomy Reviews*, 48(11-12):1413–1438.

[Eggleton, 1983] Eggleton, P. P. (1983). Approximations to the radii of roche lobes. *Astrophysical Journal, Part 1 (ISSN 0004-637X), vol. 268, May 1, 1983, p. 368, 369.*, 268:368.

[Freire and Tauris, 2013] Freire, P. C. and Tauris, T. M. (2013). Direct formation of millisecond pulsars from rotationally delayed accretion-induced collapse of massive white dwarfs. *Monthly Notices of the Royal Astronomical Society: Letters*, 438(1):L86–L90.

[Gao et al., 2020] Gao, H., Ai, S.-K., Cao, Z.-J., Zhang, B., Zhu, Z.-Y., Li, A., Zhang, N.-B., and Bauswein, A. (2020). Relation between gravitational mass and baryonic mass for non-rotating and rapidly rotating neutron stars. *Frontiers of Physics*, 15(2):24603.

[Hilditch, 2001] Hilditch, R. W. (2001). *An introduction to close binary stars*. Cambridge University Press.

[Hills, 1983] Hills, J. (1983). The effects of sudden mass loss and a random kick velocity produced in a supernova explosion on the dynamics of a binary star of arbitrary orbital eccentricity-applications to x-ray binaries and to the binary pulsars. *Astrophysical Journal, Part 1, vol. 267, Apr. 1, 1983, p. 322-333. Research supported by the US Department of Energy.*, 267:322–333.

[Hut, 1981] Hut, P. (1981). Tidal evolution in close binary systems. *Astronomy and Astrophysics, vol. 99, no. 1, June 1981, p. 126-140.*, 99:126–140.

[Iben Jr, 1967] Iben Jr, I. (1967). Stellar evolution within and off the main sequence. *Annual Review of Astronomy and Astrophysics*, 5(1):571–626.

[Iben Jr, 1991] Iben Jr, I. (1991). Single and binary star evolution. *Astrophysical Journal Supplement Series (ISSN 0067-0049), vol. 76, May 1991, p. 55-114. Pennsylvania State University-supported research.*, 76:55–114.

[Ivanova and Taam, 2003] Ivanova, N. and Taam, R. E. (2003). Magnetic braking revisited. *The Astrophysical Journal*, 599(1):516.

[Knigge et al., 2011] Knigge, C., Coe, M. J., and Podsiadlowski, P. (2011). Two populations of x-ray pulsars produced by two types of supernova. *Nature*, 479(7373):372–375.

[Lamers and Cassinelli, 1999] Lamers, H. J. and Cassinelli, J. P. (1999). *Introduction to stellar winds*. Cambridge university press.

[Larson, 2003] Larson, R. B. (2003). The physics of star formation. *Reports on Progress in Physics*, 66(10):1651.

[Lattimer and Prakash, 2007] Lattimer, J. M. and Prakash, M. (2007). Neutron star observations: Prognosis for equation of state constraints. *Physics reports*, 442(1-6):109–165.

[Lochner et al., 2004] Lochner, J. C., Williamson, L., and Fitzhugh, E. (2004). Imagine the universe!

[Lorimer, 2008] Lorimer, D. R. (2008). Binary and millisecond pulsars. *Living reviews in relativity*, 11(1):1–90.

[Massey and Olsen, 2003] Massey, P. and Olsen, K. (2003). The evolution of massive stars. i. red supergiants in the magellanic clouds. *The Astronomical Journal*, 126(6):2867.

[McKee and Ostriker, 2007] McKee, C. F. and Ostriker, E. C. (2007). Theory of star formation. *Annu. Rev. Astron. Astrophys.*, 45:565–687.

[Miller, 2010] Miller (2010). Rotation-powered pulsars. University Lecture. URL: https://www.astro.umd.edu/~miller/teaching/astr498/lecture18.pdf.

[Miskovicova, 2021] Miskovicova, I. (2021). P7: FEEDING THE MONSTER: WIND ACCRETION IN BLACK HOLE BINARIES. URL: http://www.black-hole.eu/index.php/general-public/p7-feeding-the-monster-wind-accretion-in-black-hole-binaries.ht.

[Misra et al., 2020] Misra, D., Fragos, T., Tauris, T., Zapartas, E., and Aguilera-Dena, D. R. (2020). The origin of pulsating ultra-luminous x-ray sources: Low-and intermediate-mass x-ray binaries containing neutron star accretors. *Astronomy & Astrophysics*, 642:A174.

[NASA, 2015] NASA (2015). Pulsating variable stars and the hertzsprung-russell (h-r) diagram. NASA. URL: https://chandra.harvard.edu/edu/formal/variable_stars/bg_info.html.

[Nurmamat et al., 2019] Nurmamat, N., Zhu, C., Lü, G., Wang, Z., Li, L., and Liu, H. (2019). Quark novae: An alternative channel for the formation of isolated millisecond pulsars. *Journal of Astrophysics and Astronomy*, 40:1–6.

[Ohse, 2021] Ohse, P. D. (2021). Phase transitions in millisecond pulsars.

[Onuki, 2002] Onuki, A. (2002). *Phase transition dynamics.* Cambridge University Press.

[O'Boyle et al., 2020] O'Boyle, M. F., Markakis, C., Stergioulas, N., and Read, J. S. (2020). Parametrized equation of state for neutron star matter with continuous sound speed. *Physical Review D*, 102(8):083027.

[Paczynski, 1976] Paczynski, B. (1976). Common envelope binaries. In *Symposium-International Astronomical Union*, volume 73, pages 75–80. Cambridge University Press.

[Paschalidis et al., 2018] Paschalidis, V., Yagi, K., Alvarez-Castillo, D., Blaschke, D. B., and Sedrakian, A. (2018). Implications from gw170817 and i-love-q relations for relativistic hybrid stars. *Physical Review D*, 97(8):084038.

[Paxton et al., 2010] Paxton, B., Bildsten, L., Dotter, A., Herwig, F., Lesaffre, P., and Timmes, F. (2010). Modules for experiments in stellar astrophysics (mesa). *The Astrophysical Journal Supplement Series*, 192(1):3.

[Paxton et al., 2013] Paxton, B., Cantiello, M., Arras, P., Bildsten, L., Brown, E. F., Dotter, A., Mankovich, C., Montgomery, M., Stello, D., Timmes, F., et al. (2013). Modules for experiments in stellar astrophysics (mesa): planets, oscillations, rotation, and massive stars. *The Astrophysical Journal Supplement Series*, 208(1):4.

[Paxton et al., 2015] Paxton, B., Marchant, P., Schwab, J., Bauer, E. B., Bildsten, L., Cantiello, M., Dessart, L., Farmer, R., Hu, H., Langer, N., et al. (2015). Modules for experiments in stellar astrophysics (mesa): binaries, pulsations, and explosions. *The Astrophysical Journal Supplement Series*, 220(1):15.

[Phinney, 1992] Phinney, E. (1992). Pulsars as probes of newtonian dynamical systems. *Philosophical Transactions of the Royal Society of London. Series A: Physical and Engineering Sciences*, 341(1660):39–75.

[Phinney and Blandford, 1981] Phinney, E. and Blandford, R. (1981). Analysis of the pulsar p–distribution. *Monthly Notices of the Royal Astronomical Society*, 194(1):137–148.

[Podsiadlowski, 2014] Podsiadlowski, P. (2014). The evolution of binary systems. *Accretion Processes in Astrophysics*, page 45.

[Pols, 2011] Pols, O. R. (2011). *Stellar structure and evolution.* Astronomical Institute Utrecht Nijmegen.

[Postnov and Yungelson, 2014] Postnov, K. A. and Yungelson, L. R. (2014). The evolution of compact binary star systems. *Living Reviews in Relativity*, 17:1–166.

[Pringle, 1981] Pringle, J. E. (1981). Accretion discs in astrophysics. *Annual review of astronomy and astrophysics*, 19(1):137–160.

[Reig, 2011] Reig, P. (2011). Be/x-ray binaries. *Astrophysics and Space Science*, 332:1–29.

[Romanova and Owocki, 2015] Romanova, M. M. and Owocki, S. P. (2015). Accretion, outflows, and winds of magnetized stars. *Space Science Reviews*, 191:339–389.

[Salaris et al., 2002] Salaris, M., Cassisi, S., and Weiss, A. (2002). Red giant branch stars: the theoretical framework. *Publications of the Astronomical Society of the Pacific*, 114(794):375.

[Savonije, 1978] Savonije, G. (1978). Roche-lobe overflow in x-ray binaries. *Astronomy and Astrophysics, vol. 62, no. 3, Jan. 1978, p. 317-338. Research supported by the Nederlandse Organisatie voor Zuiver-Wetenschappelijk Onderzoek and Universiteit van Amsterdam.*, 62:317–338.

[Schatz and Rehm, 2006] Schatz, H. and Rehm, K. (2006). X-ray binaries. *Nuclear physics A*, 777:601–622.

[Shapiro and Teukolsky, 2008] Shapiro, S. L. and Teukolsky, S. A. (2008). *Black holes, white dwarfs, and neutron stars: The physics of compact objects.* John Wiley & Sons.

[Tauris and Van Den Heuvel, 2006] Tauris, T. and Van Den Heuvel, E. (2006). Formation and evolution of compact stellar x-ray sources. *Compact stellar X-ray sources*, 39:623–665.

[Tauris, 2012] Tauris, T. M. (2012). Spin-down of radio millisecond pulsars at genesis. *Science*, 335(6068):561–563.

[Tauris et al., 2012] Tauris, T. M., Langer, N., and Kramer, M. (2012). Formation of millisecond pulsars with co white dwarf companions–ii. accretion, spin-up, true ages and comparison to msps with he white dwarf companions. *Monthly Notices of the Royal Astronomical Society*, 425(3):1601–1627.

[Tauris and van den Heuvel, 2023] Tauris, T. M. and van den Heuvel, E. P. (2023). *Physics of Binary Star Evolution: From Stars to X-ray Binaries and Gravitational Wave Sources*, volume 68. Princeton University Press.

[Woosley et al., 2003] Woosley, S., Heger, A., Hartmann, D., Langer, N., and Fryer, C. (2003). How massive single stars end their life.

[Zhou et al., 2017] Zhou, X., Tong, H., Zhu, C., and Wang, N. (2017). Dependence of pulsar death line on the equation of state. *Monthly Notices of the Royal Astronomical Society*, 472.